NPL Report CMSC 27/03

Report to the National Measurement System Directorate, Department of Trade and Industry

From the Software Support for Metrology Programme

Spectral characteristic modelling

By
M G Cox, P M Harris, P D Kenward
Centre for Mathematics and Scientific Computing
and Emma Woolliams
Centre for Optical and Analytical Metrology

June 2003

Spectral characteristic modelling

M G Cox, P M Harris, P D Kenward
Centre for Mathematics and Scientific Computing
and Emma Woolliams
Centre for Optical and Analytical Metrology

June 2003

ABSTRACT

The modelling of the spectral characteristics of sources and detectors in optical radiation metrology is addressed. The major objective is to provide an approach for obtaining mathematical models of spectral characteristics that are specified directly or indirectly by measurements at a set of wavelength values spanning a spectral region. A further objective is to evaluate the uncertainties associated with the models given the uncertainties associated with the measurements.

Because no wholly physical models are available, models are used that are based partly on recognised or observed physical behaviour, and include a variable number of empirical terms in order that they have the flexibility to adapt to a range of source and detector characteristics.

The effects of the slit bandwidth of the monochomators used for spectral measurement are studied in detail, because of their influence on obtaining models that are valid for the required rather than the indicated characteristics.

Application of the concepts developed is made to source and detector data.

Suggestions for future work to improve the models developed are made. Further applications in optical radiation metrology are identified that could benefit from such models.

ISSN 1471–0005

Authorised by Dr Dave Rayner,
Head of the Centre for Mathematics and Scientific Computing

National Physical Laboratory,
Queens Road, Teddington, Middlesex, United Kingdom TW11 0LW

Contents

1 Introduction

The concern here is with the modelling of the spectral characteristics of sources and detectors in optical radiation metrology. The major objective is to consider methods for obtaining mathematical models of spectral characteristics that are specified directly or indirectly by measurements at a set of wavelength values spanning a spectral region. A further objective is to evaluate the uncertainties associated with the models that arise from the fact that the measurement data has uncertainties associated with it.

The advantage of providing models and associated uncertainties for such data is that it then becomes possible to carry out many relevant tasks and to evaluate the uncertainties associated with those tasks. Typical of these tasks are (a) the provision of a smoother representation of the spectral characteristic underlying the data than implied by the data itself, and hence the ability to "interpolate" meaningfully the characteristic at any point in the spectral region, (b) the deconvolution of the data from the instrumental effects that influence the ability to measure directly the required characteristic, and (c) the evaluation of integrals based on spectral characteristics.

The modelling of sources (especially lamps) is considered first (section 2). The model developed is part physical and part empirical, being the product of a Planck function (the appropriate model for a black body) and a correction polynomial. It is shown how to construct the polynomial (section 2.1), including the choice of a suitable order for the polynomial (section 2.2). The polynomial so obtained is influenced by the colour temperature T, a parameter within the Planck function. A procedure for determining T is provided based on an operational definition given here for the colour temperature of a source (section 2.4). Applications of the approach are made to spectral irradiance measurements of lamps (section 2.5).

The above considerations require the availability of the actual spectral response of the source. In practice, *voltage* characteristics are observed, from which spectral responses are *deduced* (section 3). The considerations also depend on the provision of each spectral measurement at a point value of wavelength. In practice, an instrument provides a response that is *averaged*, according to the instrumental "slit characteristic", over a range of wavelengths centred on the nominal wavelength. It is shown how the spectral response can be determined from the voltage characteristic, and also how the measurements can be corrected to those that would have been obtained with an instrument that made *point* measurements. The relationship between this analysis and that commonly used in practice is given (section 3.1).

The modelling of the spectral responses of detectors is then discussed (section 4). Unlike sources, no simple relevant physical model is available. Therefore, a model, the exponential of a polynomial, is considered that embodies observed properties of detector responses (section 4.1). Again, it is shown how a choice for the polyno-

mial order can sensibly be made (section 4.2). Applications are made to detector response measurements (section 4.4).

Attention is paid to the limitations of the models considered and to the evaluation of the uncertainties associated with the models (especially in sections 2.3 and 4.3).

Future developments that could follow from the considerations here are indicated (section 5). They include ways in which the mentioned limitations might be addressed and hence the applicability of the models enhanced. They also include several further practical uses of the models.

2 Modelling of spectral irradiance data

Suppose that, for $i = 1, \ldots, m$, values E_i in $\mathrm{Wm}^{-2}\mathrm{nm}^{-1}$ of spectral irradiance E corresponding to values λ_i in nm of wavelength λ are available. The E_i would relate to the spectral irradiance for a reference or test source. Consideration is given in section 3 and appendix E to the manner in which the E_i might have been obtained.

Each E_i is assumed to be provided with an associated standard uncertainty $u(E_i)$. The treatment applies to mutually independent E_i. It is capable of extension to mutually dependent E_i if the associated covariances are provided. Any uncertainty associated with the λ_i is assumed to be negligible. An extension to cover non-negligible uncertainties associated with the λ_i is possible but non-trivial and not considered here.

In developing a spectral irradiance model, use is made of the fact that a black body has a spectral irradiance characteristic given by the Planck function

$$L(\lambda; T) = \frac{\alpha}{\lambda^5 (e^{\beta/(\lambda T)} - 1)} \tag{1}$$

for an appropriate value of the colour temperature T. In (1), $\alpha = 2h(c/n)^2$ and $\beta = hc/(nk)$, where h is Planck's constant, c the speed of light, n refractive index of air and k Boltzmann's constant, all positive constants.

At a given wavelength, a lamp source will emit less radiation than a black body due to the lower emissivity of the lamp filament and the finite transmittance of the bulb envelope. The use of the Planck function to model the spectral irradiance characteristic for the source would therefore exhibit systematic departures from that characteristic. In order to obtain a model that is consistent with the data (to an extent dictated by the prescribed uncertainties) the behavioural scope of the Planck function is here extended by determining an emissivity function that is appropriate for the particular characteristic. The model considered for this purpose

is the product of a (scaled) Planck function and a correction term, viz.,

$$F(\lambda;T) = CL(\lambda;T)(1 + g(\lambda)), \tag{2}$$

where $g(\lambda)$ denotes the (wavelength-dependent) correction term and C an overall scaling constant.

If such a model is viable, the influence of $g(\lambda)$ would be small (in terms of its magnitude compared with unity), but by no means negligible for the above reasons. Once such a model has been determined in any particular instance, $g(\lambda)$ can be examined to quantify this effect.

The emissivity function cannot generally be usefully determined by a physical understanding of the surface. Therefore, $g(\lambda)$ is chosen to be an empirical function, viz., a polynomial in λ.[1] This choice of model (or an approximation to it) has also been considered elsewhere [1, 18].

Now, if $g(\lambda)$ is a polynomial, $C(1 + g(\lambda))$ is also a polynomial, of the same order (degree + 1). Thus, the model (2) can be expressed as

$$F_n(\lambda;T,\mathbf{a}) = L(\lambda;T)G_n(\lambda;\mathbf{a}), \tag{3}$$

where $G_n(\lambda;\mathbf{a})$ is a polynomial correction factor of order n with adjustable coefficients $\mathbf{a} = (a_1,\ldots,a_n)^{\mathrm{T}}$. (That F also depends on n and $\mathbf{a}$ is indicated.) The function $F_n(\lambda;T,\mathbf{a})$ is referred to as a *Planck-polynomial model*.

There are (at least) two ways to proceed in providing values of T and $\mathbf{a}$:

1. Regard T and $\mathbf{a}$ as parameters to be adjusted "simultaneously" in an algorithm to determine a representation of the data by $F_n(\lambda;T,\mathbf{a})$ that is consistent with the data uncertainties. This approach is one of *nonlinear regression* or *optimisation* [14]. Because the order n of the polynomial factor $G_n(\lambda;\mathbf{a})$ is unknown *a priori*, it would be necessary to repeat the nonlinear-regression process for successive polynomial orders until a satisfactory representation was (hopefully) obtained. This approach is *not* a satisfactory way to proceed (appendix A).

2. Regard T as a parameter to be determined first by some means, thus defining the Planck function $L(\lambda;T)$ within the model $F_n(\lambda;T,\mathbf{a})$. Then, determine the polynomial factor $G_n(\lambda;\mathbf{a})$, again for successively increasing polynomial order n, until the data is (hopefully) adequately modelled by $F_n(\lambda;T,\mathbf{a})$.[2]

[1] Any continuous function can be represented arbitrarily closely by a polynomial (of sufficiently high degree)—Weierstrass' Theorem. Other empirical functions such as polynomial splines can be used. A purpose of this work is to examine the extent to which polynomials are appropriate. See section 5.5 for other empirical functions.

[2] An advantage of this approach is that determining the polynomial factor this way falls within the province of *linear* regression (i.e., with a model that is linear in its parameters).

The latter approach is adopted. The determination of $\mathbf{a}$, given T, is covered in section 2.1. The choice of polynomial order is treated in section 2.2. The associated model uncertainties are covered in section 2.3. The determination of T is covered in section 2.4 and the associated uncertainty in appendix D. Section 2.5 contains applications to spectral irradiance data.

2.1 Parameters of the Planck-polynomial model

For an estimate $\widehat{T}$ of T, consider the estimation of the coefficients $\mathbf{a}$ for a given polynomial of order n. The model residual $\epsilon_i(\mathbf{a}) = E_i - L(\lambda_i;\widehat{T})G_n(\lambda_i;\mathbf{a})$ is the signed departure of the value of the model at $\lambda = \lambda_i$ from the corresponding spectral irradiance value E_i. It is indicated as depending on $\mathbf{a}$ because, before the modelling has been undertaken, the dependence is *algebraic*. Once $\mathbf{a}$ has been estimated, *numerical* values for these residuals can be formed.

The *weighted* residual at $\lambda = \lambda_i$ is the above residual scaled by the provided standard uncertainty, viz., $\epsilon_i(\mathbf{a})/u(E_i)$. The least-squares (Gauss-Markov) estimate $\mathbf{a} = \widehat{\mathbf{a}}$ is given by solving the problem

$$\min_{\mathbf{a}} \sum_{i=1}^{m} \left(\frac{E_i - L(\lambda_i;\widehat{T})G_n(\lambda_i;\mathbf{a})}{u(E_i)} \right)^2 . \tag{4}$$

This formulation is not one of standard polynomial regression because of the presence of the values $L(\lambda_i;\widehat{T})$. It can, however, be posed as such, and corresponding software [9] utilised. Let

$$z_i = \frac{E_i}{L(\lambda_i;\widehat{T})}, \qquad u(z_i) = \frac{u(E_i)}{L(\lambda_i;\widehat{T})},$$

numerical values formed from the provided data and uncertainties. Then expression (4) can be cast as the minimisation with respect to $\mathbf{a}$ of

$$\sum_{i=1}^{m} \left(\frac{z_i - G_n(\lambda_i;\mathbf{a})}{u(z_i)} \right)^2 . \tag{5}$$

Thus, polynomial regression applied to the data (λ_i, z_i), $i = 1, \ldots, m$, with weights $1/u(z_i)$, $i = 1, \ldots, m$, delivers the estimates $\widehat{\mathbf{a}}$. The model (3), with $T = \widehat{T}$ and $\mathbf{a} = \widehat{\mathbf{a}}$, provides a candidate mathematical representation of the spectral characteristic.

For purposes of numerical stability [9], essential here to ensure valid results for polynomials of arbitrary order, $G_n(\lambda;\mathbf{a})$ is represented as

$$G_n(\lambda;\mathbf{a}) = \sum_{j=1}^{n} a_j T_{j-1}(x), \tag{6}$$

where $T_j(x)$ is the Chebyshev polynomial of the first kind of degree j in the normalised variable

$$x = \frac{(\lambda - \lambda_{\min}) - (\lambda_{\max} - \lambda)}{\lambda_{\max} - \lambda_{\min}}. \tag{7}$$

Here, $\lambda_{\min}$ and $\lambda_{\max}$ are the endpoints of the spectral region over which the model is to apply. Reasons for the specific form (7) of the linear transformation formula have been given [8].

2.2 Polynomial order in the Planck-polynomial model

Efficient processes for obtaining least-squares polynomials permit all polynomials up to a specified maximum order to be determined [9].

Let s_n denote the root-mean-square weighted residual corresponding to the obtained Planck-polynomial model of order n. It is given by

$$s_n = \left(\frac{S_n}{m-n}\right)^{1/2}, \tag{8}$$

where S_n denotes the minimising value of the sum in expression (5). If the Planck-polynomial model is generally capable of representing a spectral irradiance data set, the following behaviour is expected by analogy with the use of "pure" polynomials [9]. As n is increased through the values $1, 2, \ldots$, the values of s_n tend to decrease rapidly at first, perhaps erratically, and then to settle down to an essentially constant value.[3]

If the uncertainties $u(E_i)$ are realistic and the model is valid, the saturation level is statistically equal to unity. Thus, a simple way of selecting a value for n in this circumstance is to choose the smallest value for which $s_n \leq 1$. Should the $u(E_i)$ not be realistic, the s_n may nevertheless saturate, but to a value different from unity. If they differ from realistic values by a multiplicative factor κ, say, the s_n would saturate at the value κ^{-1}.

2.3 Planck-polynomial model uncertainties

For an estimate $\widehat{T}$ of the colour temperature T, the estimates $\widehat{\mathbf{a}}$ of $\mathbf{a}$ in the model (3) and any other quantities that depend on $\widehat{T}$ or $\widehat{\mathbf{a}}$ or both have associated uncertainties. Appendix B considers the evaluation of uncertainties associated with

1. The estimates $\widehat{\mathbf{a}}$ of the polynomial coefficients (for $\widehat{T}$ see Appendix D).

[3] If n were increased further, s_n would often start to decrease again, at some order. At this stage the model would follow the noise in the data, and thus not behave smoothly.

2. Single or several quantities that depend linearly on $\widehat{T}$ and $\widehat{\mathbf{a}}$ or both.

3. As 2, but with nonlinear dependence.

4. The special and important case of 3 when the derived quantity represents the model itself at a particular value of λ.

5. The generalisation of 4 to several values of the model, as required in integration.

6. The generalisation of 4 to the complete spectral range of concern, thus providing and *uncertainty curve* for the model as a function of λ.

The function of λ given by $u(F_n(\lambda; \widehat{T}, \widehat{\mathbf{a}}))$ constitutes a *standard uncertainty curve* for the model. The corresponding expanded uncertainty curve is $k_p u(F_n(\lambda; \widehat{T}, \widehat{\mathbf{a}}))$, where k_p is the coverage factor corresponding to coverage probability p. The *pair of curves*

$$F_n(\lambda; \widehat{T}, \widehat{\mathbf{a}}) \pm k_p u(F_n(\lambda; \widehat{T}, \widehat{\mathbf{a}})) \tag{9}$$

defines an *uncertainty swathe* for coverage probability p for the Planck-polynomial model.

An important feature of these spectrally dependent uncertainties is that they are physically meaningful for small wavelengths. The presence of the Planck function in the standard uncertainty curve and the uncertainty swathe (9) ensures that the uncertainty tends to zero as the model value tends to zero. Any possibility that the uncertainty swathe could include negative, infeasible values is avoided. Such a possibility might arise for a model not based on appropriate asymptotic behaviour.

2.4 Colour temperature definition

The approach of section 2.1 for modelling spectral irradiance data requires a suitable value for the colour temperature. Here an operational definition of colour temperature is given, and an algorithm described for determining the colour temperature of a source in accordance with that definition. The definition is based on the use of a scaled Planck function, viz., a Planck-polynomial model of order one.

Colour temperature. Given spectral irradiance data (λ_i, E_i), $i = 1, \ldots, m$, for a source, and associated uncertainties $u(E_i)$, $i = 1, \ldots, m$, determine constants $\widehat{T}$ and $\widehat{a}_1$ such that a scaled Planck function $\widehat{a}_1 L(\lambda; \widehat{T})$ provides the best approximation to this data, respecting its associated uncertainties, in the sense of least squares. Thus, $\widehat{T}$ and $\widehat{a}_1$ are determined to minimise

$$S = \sum_{i=1}^{m} \left(\frac{E_i - a_1 L(\lambda_i; T)}{u(E_i)} \right)^2 .$$

The resulting estimate $\widehat{T}$ is the colour temperature of the source.

This definition holds when the E_i are mutually independent. If the E_i are mutually dependent, a generalisation of this definition is to be used. It should be noted that the calculated value will not necessarily correspond to the actual filament temperature or to the colour temperature defined from chromaticity coordinates. However, for the purposes of this model, the temperature value chosen is not critical.

Appendix C develops a procedure for determining $\widehat{T}$ (and $\widehat{a}_1$) in accordance with this definition. Appendix D provides the standard uncertainty associated with $\widehat{T}$.

Given $\widehat{T}$, the problem of determining $\widehat{a}_1$ is identical to that addressed in section 2.1 in the case of a polynomial of order $n = 1$.

2.5 Applications to spectral irradiance data sets

The procedure considered in section 2.1 was applied to data sets representing the spectral irradiance of FEL lamps.[4] The colour temperature was first determined using the procedure in appendix C.

Figure 1 shows for lamp FEL196 the spectral irradiance data and the (scaled) Planck function (equivalently the Planck-polynomial model of order 1) computed for this data and the associated uncertainties. This data spans the spectral region from 250 nm to 2500 nm.

The standard uncertainties associated with the spectral irradiance values for this lamp were specified as

$$u(E_i) = \frac{\widetilde{u}(\lambda_i)}{100} \times E_i,$$

where $\widetilde{u}(\lambda)$ is a fractional standard uncertainty expressed in percentage terms. For this calculation the pivotal values of $\widetilde{u}(\lambda)$ in table 1 were given, together with the rule that the value at any intermediate point is given by linear interpolation.

λ in nm	250	400	800	1600	2500
$\widetilde{u}(\lambda)$ (dimensionless)	0.8 %	0.3 %	0.25 %	0.25 %	1.5 %

Table 1: Pivotal values of $\widetilde{u}(\lambda)$, fractional standard uncertainties expressed in percentage terms, associated with the FEL196 spectral irradiance data. Intermediate values are defined by linear interpolation.

The Planck function for the spectral irradiance data for this lamp was determined in accordance with the definition of colour temperature given in section 2.4. The

[4] Tungsten-halogen lamp standards bearing the ANSI designation of FEL are commonly used as transfer standards of absolute spectral irradiance from 250 nm to 2500 nm.

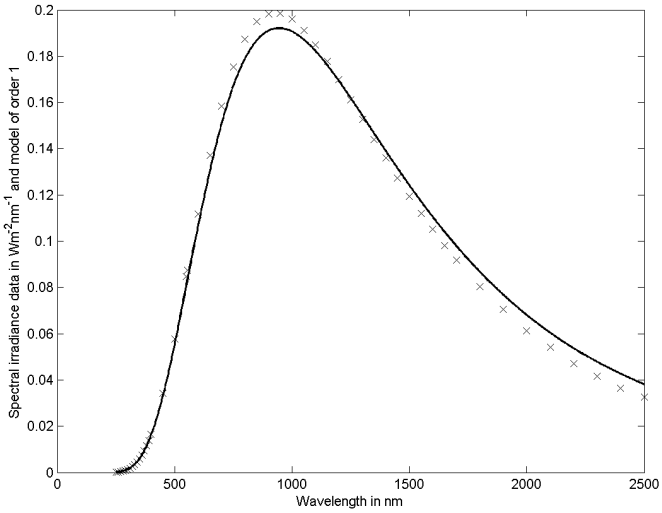

Figure 1: Spectral irradiance data for lamp FEL196 and the (scaled) Planck function (equivalently the Planck-polynomial model of order 1) computed for this data and the associated uncertainties. The Planck function was determined in accordance with the definition of colour temperature given in section 2.4.

colour temperature obtained was 3067.6 K with an associated standard uncertainty of 0.7 K. The root-mean-square weighted residual s_1 (section 2.2) for this model was 13.5. A value near unity would be obtained for a valid model, i.e., a model that was close to the data as governed by correctly specified uncertainties (section 2.1). That s_1 considerably exceeds unity implies that a (scaled) Planck function does not in itself provide an adequate representation. This fact is clear from examining figure 1, where systematic departures of the Planck function from the data are apparent.

This aspect is made more evident by a graph (figure 2) of the weighted residuals for this Planck function, viz., the values of

$$\frac{E_i - \widehat{a}_1 L(\lambda_i; \widehat{T})}{u(E_i)}, \qquad i = 1, \ldots, m.$$

Figure 3 shows the corresponding unweighted residuals $E_i - \widehat{a}_1 L(\lambda_i; \widehat{T})$. The distribution of the unweighted residuals can be interpreted as a spectral characterisation of the departure of the lamp from black-body behaviour—a representation of its emissivity function. The largest unweighted residual (in magnitude) is 4 % of the peak height of the data. That this value is an order of magnitude larger than the uncertainties associated with the bulk of the data (table 1) indicates the need to incorporate a correction to the Planck function in order to provide a valid model. Accordingly, the method described in section 2.1 was used to provide a sequence of

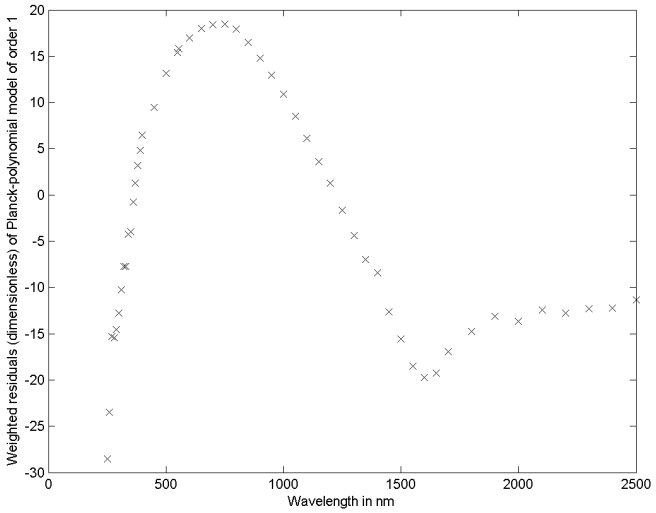

Figure 2: The weighted residuals $(E_i - \widehat{a}_1 L(\lambda_i; \widehat{T}))/u(E_i)$ for the Planck function of figure 1. Their units are dimensionless.

candidate Planck-polynomial models of successively increasing order $n = 1, 2, \ldots$ for lamp FEL196. As in that section, the root-mean-square weighted residual s_n as a function of n was used as a measure of the quality of the polynomial. Table 2 and figure 4 show these values of s_n for $n = 1, \ldots, 20$.[5]

Polynomial order n	1	2	3	4	5	6	7	8	9	10
RMS wt. residual s_n	13.5	12.0	8.6	5.7	3.9	3.0	2.3	1.6	1.2	1.0
Polynomial order n	11	12	13	14	15	16	17	18	19	20
RMS wt. residual s_n	0.9	0.9	0.9	1.0	1.0	1.0	1.0	0.9	0.9	0.8

Table 2: The root-mean-square (RMS) weighted residual s_n (non-dimensional) for the Planck-polynomial model as a function of polynomial order n for lamp FEL196.

A Planck-polynomial model of order $n = 10$ provides a satisfactory representation, not only because it is the lowest order at which the root-mean-square weighted residuals saturate for practical purposes (although there are minor improvements for higher orders), but because the value of unity (cf. section 2.2) is attained for that order.

Figure 5 shows the Planck-polynomial model for $n = 10$. Visually, the model provides a valid model for the data, exhibiting no spurious behaviour.

Figure 6 shows the weighted residuals for the Planck-polynomial model of order $n = 10$. Compare with figure 2 for $n = 1$, taking into account the different ver-

[5]The value of $s_1 = 13.5$ was mentioned above in that it corresponds to the value of this quantity in the determination of colour temperature. This value is the highest point shown in figure 4.

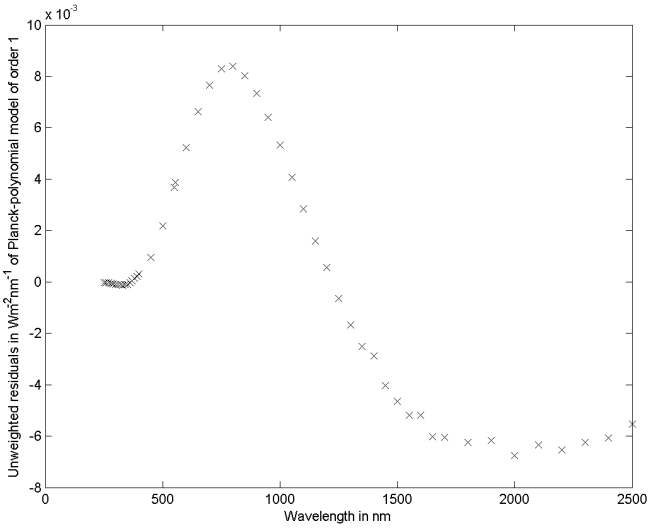

Figure 3: The unweighted residuals $E_i - \widehat{a}_1 L(\lambda_i; \widehat{T})$ for the Planck function of figure 1.

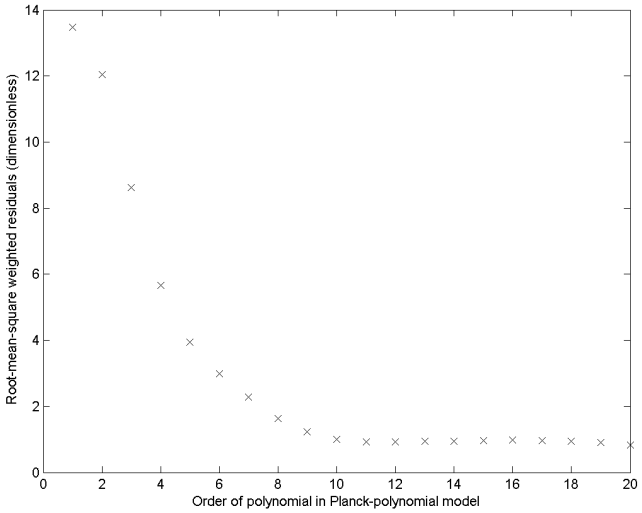

Figure 4: The root-mean-square weighted residual s_n of the Planck-polynomial model as a function of polynomial order n for lamp FEL196.

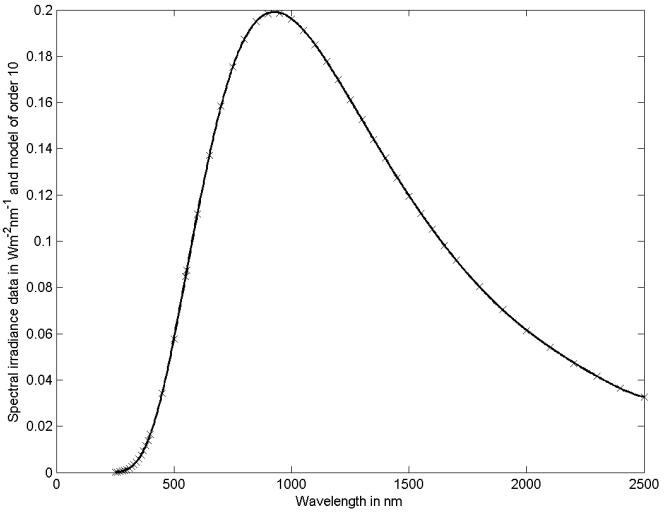

Figure 5: The Planck-polynomial model for order $n = 10$ for lamp FEL196.

tical scales. Systematic behaviour in the weighted residuals is apparent in the form of banks of positive and negative residuals, and an extreme value at $\lambda = 270$ nm. Sufficiently higher orders of polynomials do not contain such banks of residuals (although the root-mean-square weighted residual is not significantly smaller), but the extreme residual persists.

Figure 7 shows the model (unweighted) residuals $E_i - L(\lambda_i, \widehat{T})G_n(\lambda_i; \widehat{\mathbf{a}})$ (section 2.1). The largest unweighted residual (in magnitude) is 0.3 % of the peak height of the data. This value is an order of magnitude smaller than that (4 %) for the Planck-polynomial model of order 1, and is comparable to the standard uncertainties associated with the bulk of the data (table 1). This figure also shows a 95 % uncertainty swathe for the model, calculated in accordance with the treatment in section 2.3. This swathe is shown on this residual plot rather than in figure 5 for the model itself, because it would be too narrow to be seen clearly in the latter.

The 95 % uncertainty swathe has the following interpretation. Suppose that the spectral irradiance data set considered is just one realisation of many possible data sets (each with generally different random effects) that could have been measured for lamp FEL196. Suppose further that for each of these data sets a Planck-polynomial model of the same order ($n = 10$) was obtained. Consider a figure depicting all the model curves so obtained. At each wavelength within the spectral region considered it would be expected that 95 % of the values of the curves at that point would lie within the uncertainty swathe.[6]

[6]This discussion constitutes a *frequentist* interpretation. An interpretation in terms of *re-sampling* is as follows. For each value $i = 1, \ldots, m$, consider the data value E_i to be the best

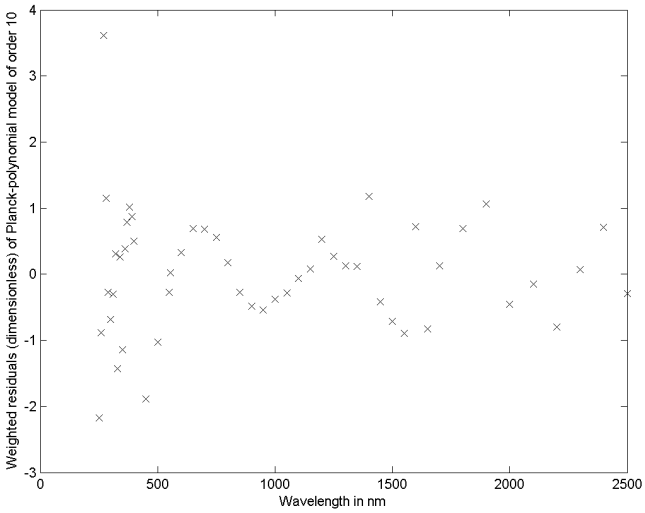

Figure 6: The weighted residuals for the Planck-polynomial model of order $n = 10$ shown in figure 5.

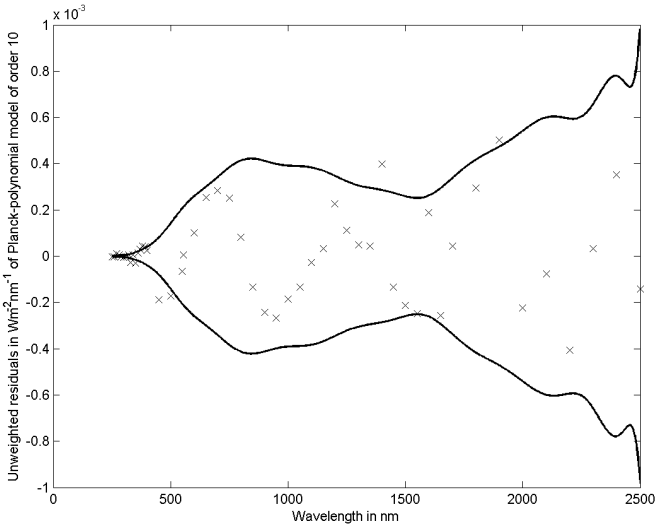

Figure 7: The unweighted residuals $E_i - L(\lambda_i, \widehat{T})G_n(\lambda_i; \widehat{\mathbf{a}}))$ (section 2.1) for the Planck-polynomial model of order $n = 10$ shown in figure 5, and a 95 % uncertainty swathe (section 2.3) for the model.

2.5.1 Further uncertainty considerations

Further analysis is possible relating to the degree of consistency of the model and the data (section 5.6). It is based on "local" analysis of the wavelength dependence of estimates of the errors in the spectral irradiance data in order to infer the uncertainties associated with the data.

3 Spectral response from an indicated voltage characteristic

The analysis in section 2 applies under the assumption that the measured spectral irradiance values E_i are *point* values, i.e., values at single wavelengths. In fact, each such value is obtained indirectly, and involves a form of averaging over a wavelength interval containing that of concern, as well as being influenced by other instrumental effects. Some background to these effects, for the *monochromator slit function*, is given in appendix E. This section considers how this aspect can be taken into account.

Spectral irradiance $E(\lambda)$ is an *energy density* that quantifies the output of a source (lamp) throughout the spectrum. The energy emitted over a range of wavelengths is the integral of $E(\lambda)$ over that range. A test source is calibrated by comparison with a reference source. Let $E_{\rm ref}(\lambda)$ denote the known spectral irradiance of the reference source and $E(\lambda)$ the required spectral irradiance of the test source. Let $R(\lambda)$ denote the unknown responsivity of the system. Let $S(\lambda_0, \lambda)$ denote the known spectral characteristic of the monochromator slit function when used at $\lambda = \lambda_0$.

Let $\widetilde{V}_{\rm ref}(\lambda)$ denote the *indicated* voltage characteristic for the reference source and $\widetilde{V}(\lambda)$ that for the test source. These characteristics are related to the above quantities by the expressions

$$\widetilde{V}(\lambda) = \int_0^\infty E(\ell)R(\ell)S(\lambda,\ell)d\ell \tag{10}$$

and

$$\widetilde{V}_{\rm ref}(\lambda) = \int_0^\infty E_{\rm ref}(\ell)R(\ell)S(\lambda,\ell)d\ell. \tag{11}$$

(available) estimate of the spectral irradiance of the source at $\lambda = \lambda_i$. Assign the Gaussian distribution $N(E_i, u^2(E_i))$ to this spectral irradiance. Carry out a large number M of re-sampling (Monte Carlo) trials. The rth such trial consists of simulating a complete spectral irradiance data set by generating a point from each of these m Gaussian distributions, associating the ith point with λ_i. Model this data set for the chosen polynomial order n in the way described. For each $\lambda = \lambda_i$ there will be M corresponding values of the model, one for each trial. The 2.5– and 97.5–percentiles of these M values would approximate the corresponding lower and upper values of the uncertainty swathe. This form of re-sampling is in fact recommended in the forthcoming guide [17] to the GUM concerned with a *general* numerical approach to uncertainty evaluation.

Equations (10) and (11) constitute a pair of coupled integral equations in the required function $E(\lambda)$ and the unknown function $R(\lambda)$. The other functions in equations (10) and (11) are known, typically by measurement.

Suppose the slit function $S(\lambda_0, \lambda)$ has support (i.e., is nonzero only over the interval) $[\lambda_0 - \Delta\lambda(\lambda_0), \lambda_0 + \Delta\lambda(\lambda_0)]$, and is normalised to have unit area. Here, the semi-width $\Delta\lambda$ of the slit function is shown as depending on the mid-point λ_0, because the width of the monochromator slits and the line spacing of the gratings will usually change from one spectral region to another, altering the slit function between regions. The dependence is not henceforth indicated explicitly.[7]

The integrals (10) and (11) become

$$\widetilde{V}(\lambda) = \int_{\lambda-\Delta\lambda}^{\lambda+\Delta\lambda} E(\ell)R(\ell)S(\lambda,\ell)d\ell \tag{12}$$

and

$$\widetilde{V}_{\mathrm{ref}}(\lambda) = \int_{\lambda-\Delta\lambda}^{\lambda+\Delta\lambda} E_{\mathrm{ref}}(\ell)R(\ell)S(\lambda,\ell)d\ell. \tag{13}$$

These equations are to be solved for $E(\lambda)$ (and $R(\lambda)$), thereby calibrating the test source through determining its spectral irradiance.

Since equation (13) contains just one unknown function, viz., $R(\lambda)$, it could be solved for that function. The substitution of $R(\lambda)$ so obtained into equation (12) would yield an equation that could be solved for $E(\lambda)$, the required spectral irradiance. This approach is not desirable, since it does not enable full advantage to be taken of the properties of the slit function.

To proceed, therefore, let

$$V(\lambda) = E(\lambda)R(\lambda) \tag{14}$$

and

$$V_{\mathrm{ref}}(\lambda) = E_{\mathrm{ref}}(\lambda)R(\lambda). \tag{15}$$

$V(\lambda)$ and $V(\lambda_{\mathrm{ref}})$ are the voltage characteristics that would be obtained for a slit function with zero bandwidth (see the analysis in appendix G).

Equations (12) and (13) can then be expressed as

$$\widetilde{V}(\lambda) = \int_{\lambda-\Delta\lambda}^{\lambda+\Delta\lambda} V(\ell)S(\lambda,\ell)d\ell. \tag{16}$$

and

$$\widetilde{V}_{\mathrm{ref}}(\lambda) = \int_{\lambda-\Delta\lambda}^{\lambda+\Delta\lambda} V_{\mathrm{ref}}(\ell)S(\lambda,\ell)d\ell. \tag{17}$$

[7] Slits with asymmetric characteristics are possible. Their analysis is more complicated and is not considered here.

It is expected, certainly for small $\Delta\lambda$, that $V(\lambda)$ will be "comparable" to $\widetilde{V}(\lambda)$ since the area under S is unity and the support of S is "small" (and similarly for the reference quantities). Each of equations (16) and (17) is a *Fredholm integral equation* of the first kind [20, p154].

The solution of such equations is generally notoriously difficult (appendix F). Appendix G shows, however, that when S (the "kernel function" in the integral equation literature) is a rectangle or a symmetric triangle, the solution can be found readily in a stable manner. The solution requires information that can be provided by a mathematical model of the voltage response data and obtained in the same manner as that for spectral irradiance in section 2.

The solution of equation (16) yields $V(\lambda)$ and that of (17) $V_{\mathrm{ref}}(\lambda)$. Then from expressions (14) and (15) the required spectral irradiance is

$$E(\lambda) = \frac{V(\lambda)}{V_{\mathrm{ref}}(\lambda)} E_{\mathrm{ref}}(\lambda). \tag{18}$$

If required, the system responsivity is obtained from expression (15):

$$R(\lambda) = V_{\mathrm{ref}}(\lambda)/E_{\mathrm{ref}}(\lambda).$$

3.1 Relationship to and extension of current practice

It was noted above that the indicated voltage response $\widetilde{V}(\lambda)$ can be expected to be comparable to $V(\lambda)$, and similarly for $\widetilde{V}_{\mathrm{ref}}(\lambda)$, in which case expression (18) gives the approximation

$$E(\lambda) \approx \frac{\widetilde{V}(\lambda)}{\widetilde{V}_{\mathrm{ref}}(\lambda)} E_{\mathrm{ref}}(\lambda). \tag{19}$$

This expression is used frequently in practice, and is typically applied pointwise, viz., at a measured wavelength value λ_i:

$$E(\lambda_i) \approx \frac{\widetilde{V}(\lambda_i)}{\widetilde{V}_{\mathrm{ref}}(\lambda_i)} E_{\mathrm{ref}}(\lambda_i).$$

From the results of appendix G, an approximation to expression (18) that is better than formula (19) for a triangular slit function can be obtained. The use of formula (48) in appendix G and its counterpart for $V_{\mathrm{ref}}(\lambda)$ in expression (18) gives

$$E(\lambda) = \left[\frac{\widetilde{V}(\lambda) - (\Delta\lambda)^2 \widetilde{V}''(\lambda)/12 + (\Delta\lambda)^4 \widetilde{V}^{iv}(\lambda)/240 - \ldots}{\widetilde{V}_{\mathrm{ref}}(\lambda) - (\Delta\lambda)^2 \widetilde{V}''_{\mathrm{ref}}(\lambda)/12 + (\Delta\lambda)^4 \widetilde{V}^{iv}_{\mathrm{ref}}(\lambda)/240 - \ldots} \right] E_{\mathrm{ref}}(\lambda). \tag{20}$$

The truncation of the series expansions in expression (20) after the terms involving $(\Delta\lambda)^2$ yields[8]

$$E(\lambda) \approx \left[\frac{\widetilde{V}(\lambda) - (\Delta\lambda)^2 \widetilde{V}''(\lambda)/12}{\widetilde{V}_{\mathrm{ref}}(\lambda) - (\Delta\lambda)^2 \widetilde{V}''_{\mathrm{ref}}(\lambda)/12} \right] E_{\mathrm{ref}}(\lambda). \tag{21}$$

The higher-order terms so deleted can often be expected to be negligible in practice. (This expectation can be tested: see points 2 and 3 below.)

The following points can be made regarding the use of the commonly used formula (19), the better approximation (21) and the "exact" expression (20):

1. The application of expression (20) requires derivatives of $\widetilde{V}(\lambda)$ in addition to just $\widetilde{V}(\lambda)$, as commonly used. If $\widetilde{V}(\lambda)$ has been modelled mathematically, as the spectral irradiance was modelled in section 2.1, these derivatives will be available by differentiating the model.

2. A valuable use of these derivatives would be to test the validity of the formula (19) commonly used. A simple way to carry out this test is to compare the values at $\lambda = \lambda_i$, $i = 1, \ldots, m$, of the better approximation (21) with those of expression (19). If for all i the differences in these values are negligible compared with the standard uncertainty $u(E_i)$, the commonly used expression (19) can be regarded as adequate. In other words, the effect of the slit function can be ignored. If this is not the case, the expression (21) can be used instead.

3. If the differences between $E(\lambda_i)$ formed from expressions (19) and (21) are not negligible, consideration should be given to the use of expression (20) with several terms of higher order.

4. Expression (21) can in principle be applied pointwise, i.e., at the measured wavelengths λ_i, using either the data values or the model values in the right-hand side. If data values are used, the resulting value of $E(\lambda_i)$ will be more influenced by the effects of the measurement uncertainties than if model values were used. The use of model values of $E(\lambda)$ is also more general in that they apply for all wavelengths within the spectral region considered, rather than just at the wavelengths at which measurements were taken.

5. A finite-difference approximation [15, p126 *et seq*] for $\widetilde{V}''(\lambda)$ is

$$\widetilde{V}''(\lambda) \approx \frac{\widetilde{V}(\lambda - \Delta\lambda) - 2\widetilde{V}(\lambda) + \widetilde{V}(\lambda + \Delta\lambda)}{(\Delta\lambda)^2},$$

[8] A similar result applies for a rectangular slit function. The only change to expression (21) is that both occurrences of the factor 12 are replaced by 6.

which can be used in expression (21) to yield

$$E(\lambda) \approx \left[\frac{\widetilde{V}(\lambda) - \frac{1}{14}\widetilde{V}(\lambda - \Delta\lambda) - \frac{1}{14}\widetilde{V}(\lambda + \Delta\lambda)}{\widetilde{V}_{\mathrm{ref}}(\lambda) - \frac{1}{14}\widetilde{V}_{\mathrm{ref}}(\lambda - \Delta\lambda) - \frac{1}{14}\widetilde{V}_{\mathrm{ref}}(\lambda + \Delta\lambda)} \right] E_{\mathrm{ref}}(\lambda). \quad (22)$$

If the uncertainties associated with the indicated values $\widetilde{V}(\lambda_i)$ are sufficiently small, the use of expression (22) at $\lambda = \lambda_i$ provides a simple means of obtaining corrected values. It would generally be preferable, however, to use values determined from a model of the data in expression (22) or (20). Moreover, the use of expression (22) at $\lambda = \lambda_i$ presents some complication at the boundaries of regions where monochromators with different slit widths are used.

6. In terms of instrument development, if a slit of sufficiently small semi-width $\Delta\lambda$ could be designed such that the terms involving $(\Delta\lambda)^2$ in expression (21) are negligible throughout the relevant wavelength range for all spectral irradiance characteristics of concern, the bandwidth effects of the slit function can be ignored.

7. To the same order of approximation as in expression (21),

$$E(\lambda) \approx \frac{\widetilde{V}(\lambda)}{\widetilde{V}_{\mathrm{ref}}(\lambda)} \left(1 - (\Delta\lambda)^2(\widetilde{V}''(\lambda) - \widetilde{V}''_{\mathrm{ref}}(\lambda))/12\right) E_{\mathrm{ref}}(\lambda). \quad (23)$$

So, if $\widetilde{V}''(\lambda)$ and $\widetilde{V}''_{\mathrm{ref}}(\lambda)$ are "sufficiently similar", which would follow from $\widetilde{V}(\lambda)$ and $\widetilde{V}_{\mathrm{ref}}(\lambda)$ being such, the commonly-used approximation (19) can be expected to be good. This is usually the case when calibrating a tungsten lamp using a similar reference lamp or a black body source operating at a similar temperature. However the use of expression (21) should be considered if the two sources have significantly different spectral shapes. Such differences can be due to the sources having considerably different colour temperatures, or because one lamp has a strongly varying spectral profile, for example that of an LED or discharge lamp, or that containing a dip caused by a change in the reflectance of a dichroic lamp.

8. Even where the two sources are the same, there will be some error introduced in the above approximation. Usually the wavelength λ_i of the individual point is assumed to be the central wavelength of the slit function. In fact, the wavelength should be calculated from the slit function weighted by the lamp output. For example, if the spectral irradiance of both sources increase with wavelength, the effective wavelength will be slightly displaced to longer wavelengths. An enhanced version of the approaches discussed would be required to account for this effect.

9. The detector spectral response data modelled in section 4 originates from laser-based calibration of filter radiometers. In that particular case the effects described here are not important, since the bandwidth of the laser

is negligibly small. However, detectors are also often calibrated using a broadband source with a monochromator. In this case the results described in this section are relevant. The detector is calibrated by direct comparison with a reference detector. The signal measured in each detector is given by equations comparable to equations (10) and (11):

$$V(\lambda) = \int_0^\infty R(\ell)K(\ell)S(\lambda,\ell)d\ell, \quad V_{\mathrm{ref}}(\lambda) = \int_0^\infty R_{\mathrm{ref}}(\ell)K(\ell)S(\lambda,\ell)d\ell,$$

where $R(\lambda)$ and $R_{\mathrm{ref}}(\lambda)$ are the responsivity functions of the test and reference detectors, $K(\lambda)$ is the radiance of the source used to transfer the calibration and $S(\lambda_0, \lambda)$ is the slit function of the monochromator. Filter radiometers are typically calibrated against trap detectors. If the filter radiometer has a narrow bandwidth, and sharp cut-on and cut-off, the width of the monochromator slit function could be of the same order as the filter radiometer bandwidth. Since trap detector responsivities are only slowly varying with wavelength, the reference detector may be considered spectrally flat over the region of interest. In this case significant errors would be introduced by using the straightforward approximation.

4 Modelling of detector response data

For detectors there would appear to be little physical basis on which to build a suitable model. The spectral characteristic typically seems to decay exponentially at its extremes, although the tail behaviours are not generally mirror images of each other. Therefore a model is investigated that has the potential to reproduce some of the properties of detector response that are observed in practice.

Denote the spectral response data by (λ_i, y_i), $i = 1, \ldots, m$, and the standard uncertainties associated with the y_i by $u(y_i)$, $i = 1, \ldots, m$. As with the spectral irradiance data (section 2), any uncertainty associated with the λ_i is taken as negligible, and the y_i are taken as mutually independent.

4.1 Parameters of the exponential-polynomial model

For an initial family of models of a detector, the function

$$F_n(\lambda; \mathbf{a}) = \exp(G_n(\lambda; \mathbf{a})), \tag{24}$$

where $G_n(\lambda; \mathbf{a})$ is a polynomial of order n in λ, as in section 2.1, is used. The motivation for this choice is as follows. Let n denote the order (degree + 1) of $G_n(\lambda; \mathbf{a})$. The function F_3 is the exponential of a quadratic polynomial in λ. If the coefficient of the quadratic term in this polynomial is negative, the resulting F_3

is another way of expressing a (scaled) Gaussian curve in λ, the familiar symmetric bell-shaped function. Thus, when $n = 3$, F includes a Gaussian curve as a particular case. For larger values of n, F_n can behave asymmetrically. F_n can also exhibit various degrees of kurtosis. It can even have two or more distinct or overlapping peaks. Thus, in principle, this class of functions has the potential to be considered for modelling detector data. A member of this class is termed an *exponential-polynomial model*.

Since the natural logarithm of the model (24) is the polynomial $G_n(\lambda; \mathbf{a})$, modelling the natural logarithms of the data values by $G_n(\lambda; \mathbf{a})$ would provide a possible approach. However, such an approach distorts the uncertainty structure of the data. Consider a measured data value y that differs from the actual value y^*, say, by an additive amount δy, i.e., $y = y^* + \delta y$. Taking logarithms of the data would involve forming quantities typified by $\log y = \log(y^* + \delta y)$. Thus, the additive amount δy enters the transformed data in a nonlinear manner, and dealing with this information inappropriately could have a deleterious effect on the solution obtained. Certainly, the evaluation of the resulting uncertainties would be compromised.

It is well recognised [7] that such problems can be handled in a more valid manner. Two approaches are considered here and one recommended following a discussion of their merits.

First, similarly to the treatment in section 2.1, the correct statement of the modelling problem is to minimise, with respect to the n coefficients $\mathbf{a}$ of $G_n(\lambda; \mathbf{a})$, the weighted residual sum of squares

$$S_n = \sum_{i=1}^{m} \left(\frac{e_i}{u(y_i)} \right)^2, \tag{25}$$

where

$$e_i = y_i - \exp(G_n(\lambda_i; \mathbf{a})). \tag{26}$$

This is a nonlinear least-squares problem in the coefficients $\mathbf{a}$ and in principle can be solved using recognised algorithms [14]. In fact, it is a rather special such problem, having particular structure because of the manner in which $\mathbf{a}$ enters. An algorithm can be designed that accounts for this structure. Candidate solutions would be obtained for a succession of increasing values of n, one of these solutions being selected (section 4.2).

A second approach is based on taking logarithms as indicated above, but compensating, at least partially, for the indicated effect of doing so. Form the transformed ordinates $z_i = \log y_i$ and the transformed uncertainties $u(z_i) = u(y_i)/y_i$.[9] Model the data (λ_i, z_i) with associated uncertainties $u(z_i)$, $i = 1, \ldots, m$, by polynomi-

[9] See point 1 below for the exceptional case $y_i \leq 0$.

als $G_n(\lambda; \mathbf{a})$ of successively increasing order n. The solution to this problem better approximates that of the original problem.

The justification is as follows. The problem solved can be expressed as the minimisation with respect to $\mathbf{a}$ of the weighted residual sum of squares

$$\widetilde{S}_n = \sum_{i=1}^{m} \left(\frac{d_i}{u(z_i)} \right)^2, \tag{27}$$

where

$$d_i = z_i - G_n(\lambda_i; \mathbf{a}).$$

For the problems of minimising S_n and minimising $\widetilde{S}_n$ to be equivalent, $u(z_i)$ must be chosen such that

$$\frac{d_i}{u(z_i)} = \frac{e_i}{u(y_i)},$$

i.e.,

$$u(z_i) = \frac{d_i}{e_i} \times u(y_i) = \frac{\log y_i - G_n(\lambda_i; \mathbf{a})}{y_i - \exp(G_n(\lambda_i; \mathbf{a}))} \times u(y_i).$$

The right-hand side involves $G_n(\lambda; \mathbf{a})$, which depends on $\mathbf{a}$, the polynomial coefficients. However, the application of de l'Hôpital's rule, assuming the residuals are small, gives

$$u(z_i) \approx \frac{1/y_i}{1} \times u(y_i) = \frac{u(y_i)}{y_i}. \tag{28}$$

Thus, by using fractional rather than absolute uncertainties, a *linear* problem can be solved for $\mathbf{a}$.

Further points are:

1. If any $y_i \leq 0$ exclude it from the analysis.[10] Such a value should only arise as a consequence of uncertainty of measurement.
2. Some detector data has complicated behaviour, implying that a high order of polynomial might be required.
3. As n increases and the residuals generally become smaller, the solution obtained becomes closer to that of the nonlinear least-squares problem.

Practical experience in other areas in working with polynomial models that constitute transformations of models such as function (24) is that a polynomial order that is sometimes one or rarely two greater may be required compared with working with nonlinear models. However, greater simplicity results from working with a family of models.

[10] A negative value could possibly arise depending on the nature of the instrumentation; a "perfect" instrument would provide a non-negative value. If such values are taken as zero, the corresponding weights (the relevant values of $u^{-1}(z_i)$—see expression (28)) would be zero, and thus have *no influence* on the modelling.

4.2 Polynomial order in the exponential-polynomial model

The determination of an appropriate order of polynomial follows closely the treatment for spectral irradiance modelling (section 2.2). The differences are that each successive polynomial determined relates to the minimisation of $\widetilde{S}_n$ in expression (27) for a specific polynomial of order n rather than that of expression (25). However, the actual least-squares problem is solved only approximately (although accurately for small residuals d_i—point 3 above). Hence, the *actual* root-mean-square residuals should be calculated from formula (25), with e_i given by formula (26) evaluated at $\mathbf{a} = \widehat{\mathbf{a}}$.

4.3 Exponential-polynomial model uncertainties

In section 2.3 (and appendix B) the uncertainties associated with modelling data by a pure polynomial model $G_n(\lambda; \widehat{\mathbf{a}})$ were given. These uncertainties took the form of an uncertainty matrix $V_{\widehat{\mathbf{a}}}$. Formula (35) was stated, which expressed $V_{\widehat{\mathbf{a}}}$ in terms of the uncertainty matrix V_{E} for the data. The covariance matrix for the Planck-polynomial model was then given by modifying the Jacobian matrix occurring in expression (35) to account for the presence of the Planck function as a multiplicative factor.

For the detector model, rather than the product of a Planck function and a polynomial, the exponential of a polynomial (24) is used. The resulting problem was shown to be identical, to first order, to that of working with a pure polynomial model, but applied to the logarithms of the data, and with data uncertainties equal to $u(y_i)/y_i$ rather than $u(y_i)$. The modification that needs to be made is therefore straightforward.

The most important quantity is the standard uncertainty $u(F_n(\lambda; \widehat{\mathbf{a}}))$ associated with the value $F_n(\lambda; \widehat{\mathbf{a}})$ of the exponential-polynomial model at λ. Application of the law of propagation of uncertainty to function (24) gives

$$u(F_n(\lambda; \widehat{\mathbf{a}})) = F_n(\lambda; \widehat{\mathbf{a}}) u((G_n(\lambda; \widehat{\mathbf{a}})).$$

Thus, the standard uncertainty associated with the value of the exponential-polynomial model is readily evaluated as the product of that value and the standard uncertainty of the polynomial part of that model. The latter is delivered by the polynomial modelling algorithm, as considered for source modelling in section 2.1. An expanded uncertainty and hence a coverage interval corresponding to, say, a 95 % coverage probability then follows as before.

4.4 Applications to detector response data

The procedure considered in section 4.1 was applied to data sets representing detector response. The data uncertainties were taken initially as $u(y_i) = 0.01y_i$, i.e., corresponding to a relative uncertainty of 1 %, although a cut-off value equal to the smallest data y-value was then applied. Thus, the values

$$u(y_i) = \max\left(0.01y_i, \min_r y_r\right), \qquad i = 1, \ldots, m,$$

were used.

One detector response data set, identified as DTCT710A, is shown in figure 8. The function represented by the data appears as an asymmetric peak, but exhibits some Gaussian-like behaviour. An exponential-polynomial model, for an appropriate order of polynomial, might therefore be expected to provide an acceptable representation.

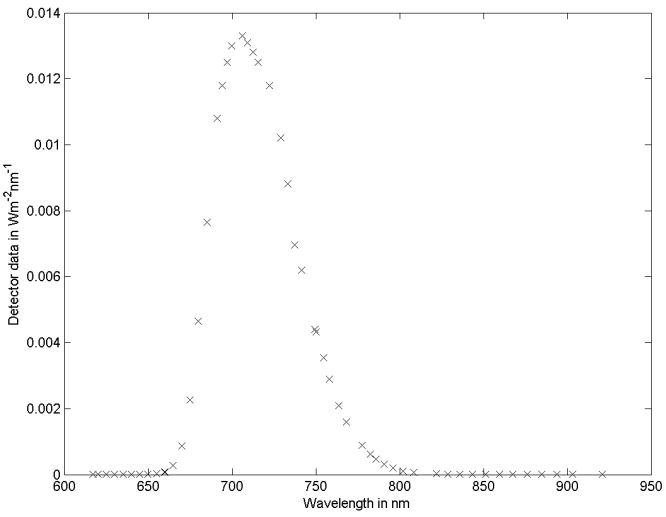

Figure 8: Spectral response data for detector DTCT710A.

In accordance with the approach considered in section 4.1, models having polynomial orders from one to 45 were constructed for the DTCT710A data. The number of data points is 51, so order 45 is close to the maximum possible for such a model. The resulting root-mean-square weighted residuals are shown in figure 9. This figure is shown on a log scale, because the root-mean-square weighted residual decreases by nine orders of magnitude over these polynomial orders. Only at a polynomial order of approximately 40 have the root-mean-square weighted residuals shown a sign of saturating, to a value of 1.4 (compared with the statistically

expected value of unity).[11]

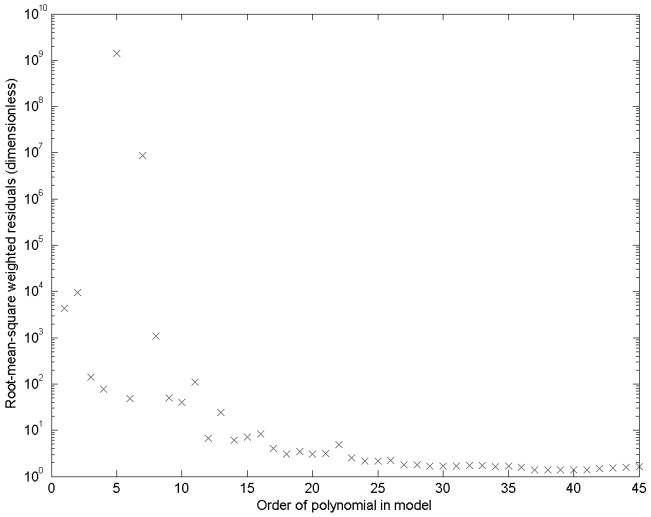

Figure 9: The root-mean-square weighted residual of the exponential-polynomial model as a function of polynomial order for detector DTCT710A. This figure is shown with the response variable on a log scale, because the values of the root-mean-square weighted residuals vary by nine orders of magnitude.

The exponential-polynomial model of order 40 is totally unacceptable, oscillating wildly between the data points. The reasons for such behaviour are well recognised for pure polynomial models [16]. The conclusion is that the model is inadequate for this type of data (or *vice versa*), at least to obtain a solution that is consistent with the data uncertainties.

In order to demonstrate further that a polynomial of reasonably high order (within the class of exponential-polynomial models) is necessary, figures 10 and 11 show the model corresponding to polynomial order 10. The first of these figures depicts the model polynomial of order 10 for the logged data and the second the corresponding exponential-polynomial model. The model has evident deficiencies in the neighbourhood of the peak. Moreover, the root-mean-square weighted residual for this order is 40, a very high value.

Figure 12 shows the unweighted residuals $y_i - F(\lambda; \widehat{\mathbf{a}})$ for the exponential-polynomial model of order 10. The figure also shows the uncertainty swathe for the model. Because they correspond only to large negative values of the logged data, the polynomial model inadequacies in figure 10 for wavelengths less than 645 nm

[11] The root-mean-square weighted residual in fact "stabilises locally" for several ranges of lower polynomial order, to improve thereafter. The dangers of terminating the modelling at too low a polynomial order are apparent.

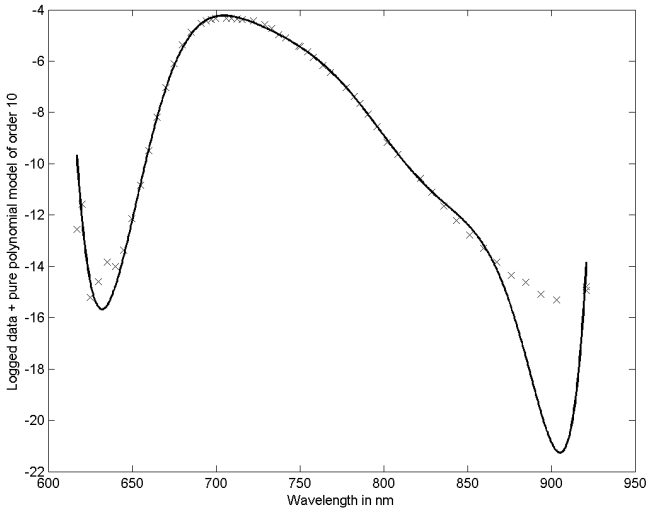

Figure 10: The polynomial model of order 10 for the logged data for detector DTCT710A.

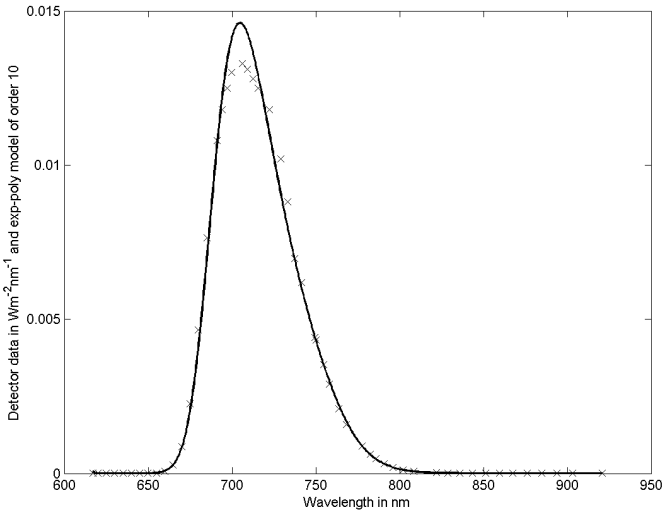

Figure 11: The exponential-polynomial model of order 10 for detector DTCT710A.

and greater than 830 nm are totally negligible for the corresponding exponential-polynomial model. Compare the unweighted residuals for this model in figure 12.

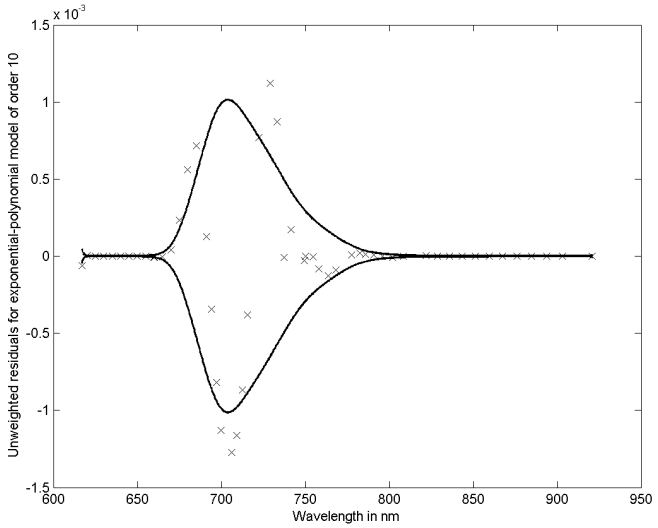

Figure 12: The unweighted residuals $y_i - F(\lambda; \widehat{\mathbf{a}})$ for the exponential-polynomial model of order 10 for detector DTCT710A.

The exponential-polynomial model of order 20 (figure 13) is a considerable improvement over that for order 10, particularly in its ability to represent the peak. The root-mean-square weighted residual for this order is 3.1. The corresponding polynomial model for the logged data (figure 14) demonstrates clearly spurious behaviour near one end of the spectral range. This effect is not noticeable in figure 13 as a consequence of the exponentiation as explained above.

An instance of data that is even more difficult to model is shown in figure 15. It represents the measured response of detector 800W10HB.

If polynomials prove to be ineffective (for some data sets), a polynomial spline function could be used in place of the polynomial in the Planck-polynomial model for sources, i.e., a Planck-spline would be used. Similarly, an exponential-spline model could be used for detectors. Polynomial splines have already proved to be invaluable in a range of metrology applications [9]. Splines, however, are more difficult to use because a choice of knots (here the values of λ where adjacent polynomial pieces join) has to be made. A discussion of the considerations involved is available [12]. An illustration of the capability of an exponential-spline model to represent the detector data of figure 15 is given in figure 16. A polynomial spline of order four with 100 uniformly-spaced knots was used. Although there are many data points (some 450 in all), exponential-polynomial models are far less suitable for this data than the exponential-spline model shown.

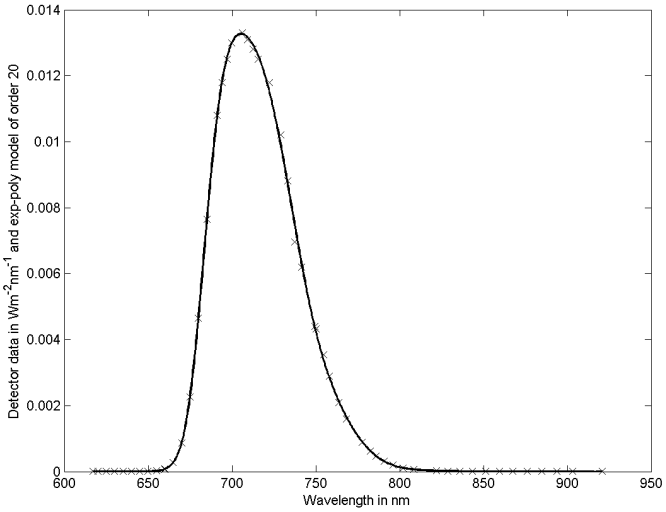

Figure 13: The exponential-polynomial model of order 20 for detector DTCT710A.

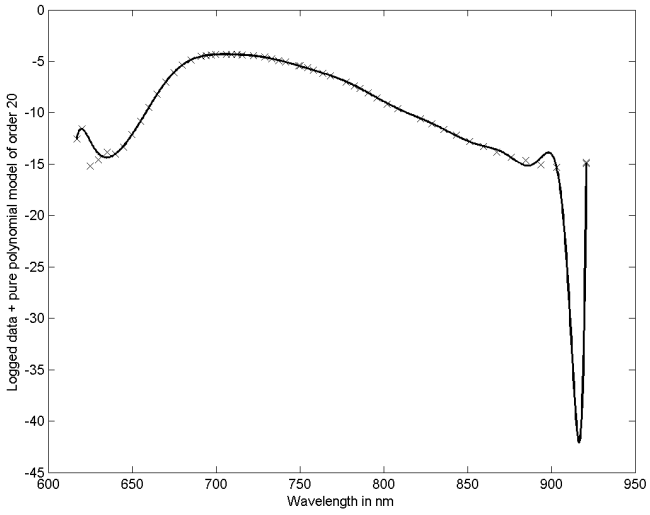

Figure 14: The polynomial model of order 20 for the logged data for detector DTCT710A.

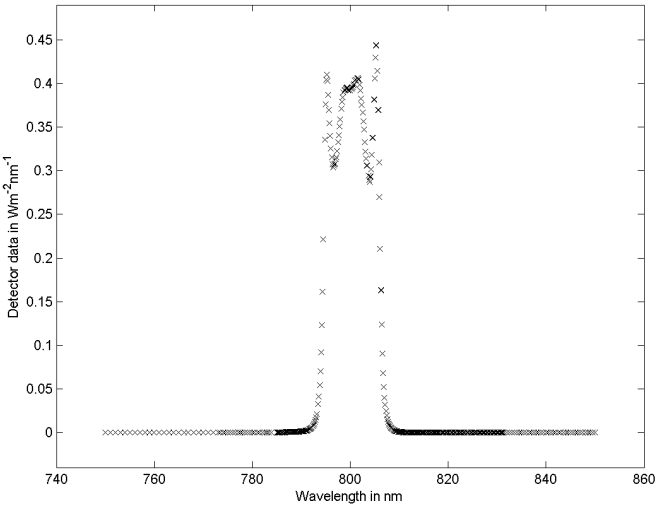

Figure 15: Response data for detector 800W10HB.

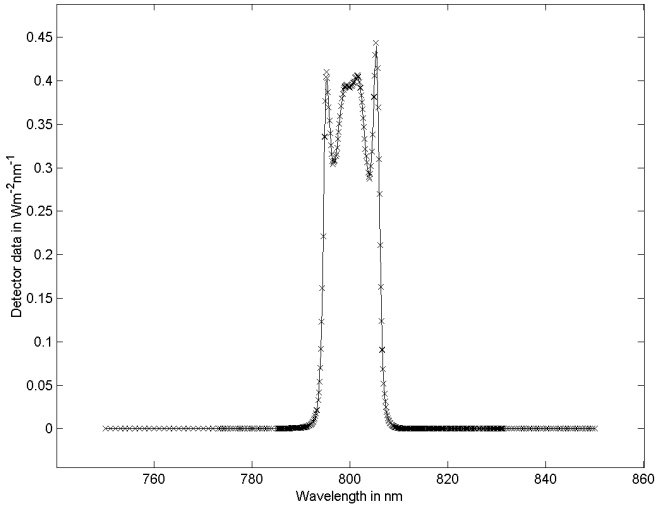

Figure 16: Exponential-spline model of order four and 100 uniformly spaced knots for the response data for detector 800W10HB.

5 Future developments

This work has developed models for the spectral irradiance of a source or the spectral responsivity of a detector. The models constitute curves that provide smooth representations of the measurement data and are defined throughout the spectral region considered. In addition, the models provide associated uncertainties throughout this region. The models can treat measurements taken with monochromators because they are able to account for the slit functions of these instruments. Two types of slit function—rectangular and triangular—were addressed.

It is commonly required to interpolate data between the measured points, either to allow comparison with another source measured at different wavelengths, or to compare an older measurement at one set of wavelengths with a newer measurement at another. It may be necessary to use the source at wavelengths other than those at which it was calibrated. The models should be useful in their current form for this work. They have limitations, however.

This section discusses potential uses of the models beyond the above considerations. Also, the models can be improved to eliminate or at least reduce some of the limitations and extend their applicability. Sections 5.1–5.6 discuss improvements to the models and sections 5.7–5.11 potential uses.

5.1 Use of the raw data

The data originally supplied by NPL's Optical Radiation Metrology Group was the calculated lamp irradiance and filter radiometer responsivity data. This data had been treated using the method discussed in section 3.1 and equation (18), from a comparison between a test and a reference source or detector.

However, the discussion in section 3.1 has shown the need to take the raw measured voltage data into account, since differences between the test and reference source need to be understood, along with the spectral variation of the system responsivity over the wavelength range of the slit function.

A more advanced model would work directly with the raw data, rather than the calculated spectral irradiance or responsivity. The basic tools for this more advanced model were indicated in section 3.

5.2 Arbitrary slit functions and wavelength uncertainty

It has been assumed that the measurements are made either at a precisely known wavelength, i.e., of negligible bandwidth (laser-based calibration of detectors),

or with a monochromator having a triangular slit function centred on a precisely known wavelength.

The examples considered did not depend strongly on this assumption. The detectors were filter radiometers calibrated using a laser-based source. The sources were calibrated with the NPL Spectral Radiance and Irradiance Primary Scales (SRIPS) facility, where a quality monochromator ensures that the wavelength uncertainty is negligible.

However, to extend the range of measurements to which the methods considered can be applied, it will be necessary to consider the use of a monochromator having a slit function that is not perfectly triangular and a central wavelength that is imprecisely known. These two effects can be considered as contributors to uncertainty and need to be treated together because the integrated nature of the measurements, as described by expressions (10) and (11) will affect both of them. The effect of an imprecisely known wavelength is greater in regions where there are sharp features in the responsivity of the system, for example, sudden changes in grating reflectance, and when the two sources behave differently with wavelength.

A further extension is the use of a continuous scan monochromator. Instead of taking measurements as above, the monochromator grating is slowly but continuously turned and measurements are taken by integrating over a time period effectively to select a certain range of wavelengths in each period. Such monochromators are commonly used for sources with sharp spectral features (a fluorescent lamp is such a source) to resolve fully the peaks and account for them. However, the slit function here is a mixture of the real slit function of the monochromator and the scanning. It will therefore have a complex shape. Sources with sharply varying spectral peaks are most influenced by a slit function, especially as they are calibrated with respect to a smoothly varying tungsten or black body source.

5.3 Random and systematic effects

The approaches considered have assumed that the measurements at the various wavelength values are mutually independent. This is a reasonable assumption for a range of sources and detectors. However, for cases in which there are appreciable systematic effects, the use of these approaches would be expected to provide uncertainties associated with the model of the characteristic that are optimistically small. Further work is needed to model source and detector responses in the presence of both random and systematic effects. The consequence of the latter would be to introduce correlation effects, account of which would need to be taken in order to generate valid results.

5.4 Discontinuities in indicated spectral characteristics

It is sometimes impossible to make "absolute" measurements in all, or even any, spectral regions using a particular measurement facility. In this case relative measurements are made. As a consequence, the spectral shape of the irradiance or responsivity will be correct, but the entire curve will need to be scaled by a constant to calculate the absolute irradiance or responsivity.

Further, for a large range of wavelengths, measurements will typically be made differently in each of a number of overlapping spectral regions. If relative measurements are made in some or all of the regions, there may be artificial "jumps" between regions because of the different scaling factors involved. If at least one region contains absolute measurements, it should be possible to match other spectral regions to them in order to model the characteristic overall. If none of the regions contains absolute measurements, the relative overall shape could be achieved by matching to any of the spectral regions, with the absolute measurement provided subsequently, using a different technique such as that indicated in section 5.8.

Future work could cover these effects. One approach would be to consider a model that contained additional parameters to represent the jumps. Each spectral region that had been measured in a relative manner would have an associated unknown multiplicative constant. If those constants could have been applied to the data prior to modelling it, the resulting representation would be expected to be smooth as required.

These parameters can be estimated by including them within the model, and determining them as part of the least-squares procedure. The basic concept has previously been applied in a different context as part of a model consisting of a (pure) polynomial with a number of additive discontinuities [2].

5.5 Model generalisation and experimental design

Although this work has demonstrated the ability of Planck-polynomial models to represent source characteristics and exponential-polynomial and exponential-spline models to represent detector characteristics, it is necessary to gain further experience with the use of these models. It would be important as part of future work to apply the modelling procedures discussed to a wider range of source and detector characteristics in order to determine the extent of their applicability. Almost inevitably there will be classes of sources and detectors requiring models with differing features. It would be necessary to adapt or provide variants of the models to cater for these features. A valuable outcome would be a classification of the main types of source and detector characteristics and the corresponding model types, with recommendations on the respective modelling procedures to be applied.

There are advantages in maximising the use of Planck-polynomial models for representing source characteristics and exponential-polynomial models and exponential-spline models for detector characteristics. So, it is appropriate to understand the nature of the occasional ineffectiveness of such polynomial-based models. The commonest instance where an unacceptable solution might be obtained is when an order of polynomial is required to model the characteristic that is too high for the data available to define it adequately. It is recognised [16] that unless the data spacing is sufficiently small (here with respect to λ), especially near the endpoints of the (spectral) range, the model might exhibit undesirable oscillations for polynomials of higher order.

Figure 17 exemplifies this phenomenon. It shows the Planck-polynomial model of order 20 for the FEL196 data. In the region 2400–2500 nm the model has an unacceptable trough, with a consequential damped oscillation for wavelengths less than 2400 nm.

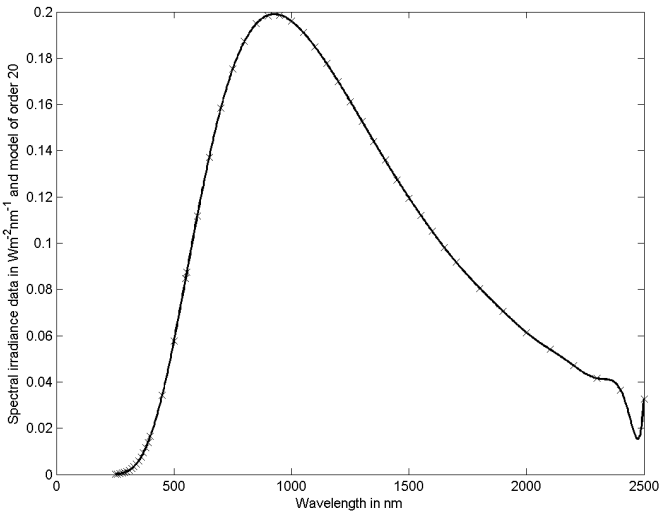

Figure 17: The Planck-polynomial model of order 20 for the FEL196 data.

Were additional measurements taken and used in the modelling this phenomenon would be avoided. To demonstrate this aspect an *artificial* data point was constructed at $\lambda = 2450$ nm, simply by linear interpolation between the values of E_i at $\lambda = 2400$ nm and 2500 nm. The uncertainty associated with this point was assigned in the same manner as in section 2.5, using table 1. The Planck-polynomial model of order 20 for the FEL196 data augmented in this manner is shown in figure 18.

In fact, models of all orders up to 20 were constructed for this augmented data. The root-mean-square weighted residuals agreed in all cases to within 0.1 $\mathrm{Wm}^{-2}\mathrm{nm}^{-1}$

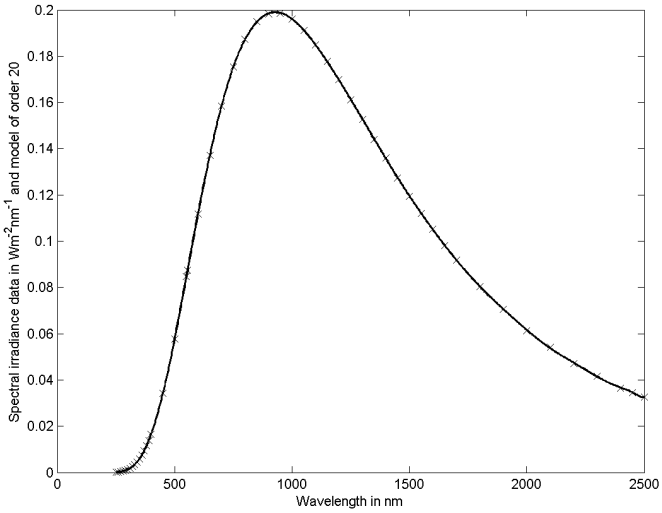

Figure 18: The Planck-polynomial model of order 20 for the FEL196 data augmented by an artificial measurement at $\lambda = 2450$ nm.

of those in table 2 for the original data.

Although a model of order 20 was unnecessary for the FEL196 data, a model of such an order or a higher order might be required for some sources.

The above considerations indicate that the use of carefully chosen additional measurements could be beneficial in obtaining valid models of spectral characteristics. Although taking more measurements increases the expense, consideration could also be given to a reduction in the number of measurements in spectral regions where the data is not critical to the modelling. One such region is 250–400 nm, where the measurements have a spacing of 10 nm (compared with that of 100 nm at the right-hand end of the spectral range). (The fine spacing might of course be important for other purposes.)

For "pure" polynomial modelling, i.e., modelling data having equal uncertainties, an ideal set of wavelengths would be given by the "Chebyshev points" [6]. These points are uniformly spaced, not in wavelength, but in a transformed variable. A set of N Chebyshev points in a variable x covering the interval $[-1,\ 1]$ is given by

$$x_k = \cos \pi(k-1)/(N-1), \qquad k = 1, \ldots, N.$$

Thus, these points are uniformly spaced in a variable θ in the interval $[0,\ \pi]$. See figure 19.

The corresponding wavelength values λ_k are given by linearly transforming the

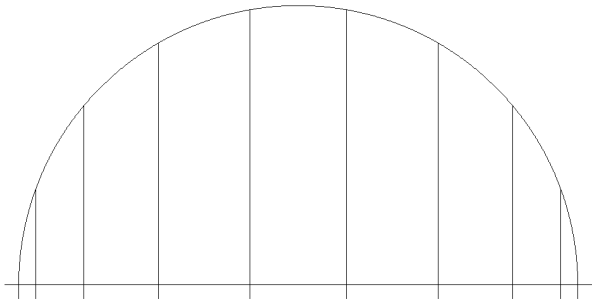

Figure 19: The Chebyshev points for order $N = 10$. N points are uniformly spaced on a unit semi-circle defined for polar angles between zero and π. The Chebyshev points are given by projecting these points onto a horizontal axis.

values x_k in the variable x to the variable λ, according to

$$\lambda_k = \frac{\lambda_{\min}}{2}(1 - x_k) + \frac{\lambda_{\max}}{2}(1 + x_k),$$

where $[\lambda_{\min},\ \lambda_{\max}]$ denotes the spectral region of concern. The use of a value of N at least as large as the highest order of polynomial used, and such that spectral values measured at these values of λ_k represent adequately the response, can be expected to give an acceptable polynomial model for some order n less than N. The use of Chebyshev points for practical polynomial curve fitting has previously been emphasised [16].

A good strategy would be to take measurements at N Chebyshev points (where N is sufficient as above), supplementing these values by measurements taken in critical regions, e.g., to define adequately a peak. It may only be necessary to take measurements in the usual way and supplement them by measurements at the first few and last few of these N Chebyshev points.

Even if actual measurements at the Chebyshev points could not be obtained, artificial data could be used as mentioned above. One way to generate artificial points is to evaluate at these points an approximant or interpolant for the data. An approximant might be based, for example, on the use of local polynomials (section 5.6). An interpolant could be defined by the piecewise linear function joining the (ordered) data points. The use of artificial points, although decidedly inferior to the use of actual measurements, can help to enforce acceptable model

behaviour.

The use of additional artificial data at the so-called “Chebyshev points” to improve the quality of polynomial models has been applied in this work to detector data. The results obtained by augmenting the data by artificial values at Chebyshev points near the range endpoints are promising. The values at these points were obtained by piecewise linear interpolation.

Figure 20 indicates what is possible. It corresponds to an exponential-polynomial model of order 50 (*sic*) based on the DTCT710A detector data augmented by 10 Chebyshev points near each end of the spectral range.

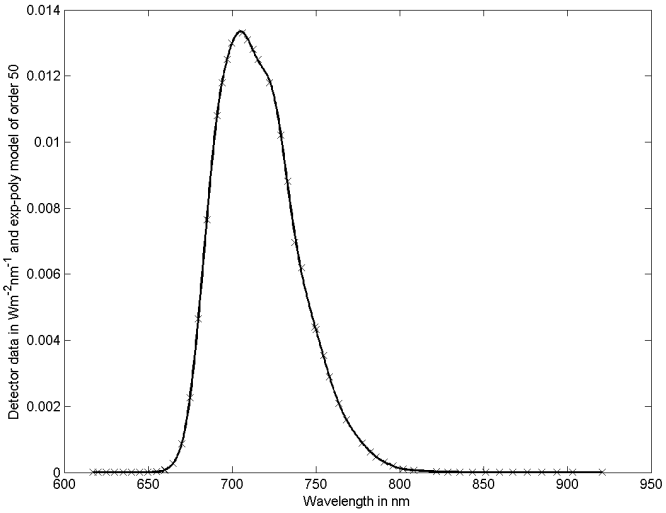

Figure 20: The exponential-polynomial model of order 50 for data for detector DTCT710A augmented by artificial points.

The difficulty of modelling this data arises from the presence of the elbow in the characteristic to the right of the peak. Generally, local features such as this require a high order of polynomial that could not be obtained with a relatively small quantity of data. Polynomial splines, although harder to use, have a much greater ability to model such features. The difficulty is largely overcome through the use of artificial points. However, although the approach appears to be valuable in terms of modelling in the sense of obtaining a good approximation, much needs to be learned about the nature of the uncertainties associated with such models.[12]

[12] A practical attitude to take to such approaches is as follows. Regardless of the method by which a model is obtained, the parameters of that model will be functions, perhaps complicated functions, of the problem data and possibly of other data. As such, the uncertainties associated with these parameters will depend on that data and on the uncertainties associated with that data. When artificial data is generated, e.g., by piecewise linear interpolation, the uncertainties associated with *that* data can be obtained by applying the law of propagation of uncertainty [4]. Mutual dependencies between

Exponential-spline models have been applied successfully for the above detector data, but their use is less automatic than polynomial-based models. Also see section 4.4.

For Planck-polynomial modelling for data with arbitrary associated uncertainties, the best points would be different from those above. Their values would depend of the colour temperature T and the uncertainties, but could be computed. The details of the computation would require some research.

5.6 "Local" analysis and uncertainty evaluation

A form of validation of response data such as that for sources and detectors is possible. In particular, the use of "local" analysis permits estimates of the data uncertainties to be made for comparison with those specified. The concept requires development and generalisation, but an indication is given of its potential through the use of the spectral irradiance data for lamp FEL196 (section 2.5) The analysis uses local polynomial models. Consider the data points arranged so that the wavelength values form an increasing sequence. For each of these points (apart from the first few and the last few), consider the subset of points given by the point itself and a small number to the left and and the same number to the right. Model the subset by a low-order polynomial, attaching the same weight to each point in the subset, taking the root-mean-square residual of the model as an estimate of the standard uncertainty of the data at and in the neighbourhood of the central point.

The approach relies on the statement that over a small interval any sufficiently smooth function can be modelled by a polynomial of low order. See the footnote in section 2 concerning Weierstrass' Theorem. For the FEL196 data the polynomial order was taken as three and the number of points each side of the central point as two.[13] Figure 21 depicts by crosses the standard uncertainties obtained plotted against the corresponding values of λ.

These standard uncertainties could be taken as those to be used in modelling the data, especially if it is difficult to provide appropriate values. However, values are not provided by this means for the first two and the last two data points (although an extension of the approach could furnish such values). More importantly, the values are influenced by the vagaries of local polynomial regression: the small number (five) of points used implies that the estimate so obtained of the standard

the original and the artificial data will exist because of the manner of generation. If implemented correctly, the law of propagation of uncertainty will account for such dependencies. Hence, the uncertainties associated with whatever the rule for establishing and using the artificial data may be can be taken into account. Because the data is artificial there is no possibility that it could add information in terms of reducing uncertainties over what could be deduced from the raw data alone. However, as noted, it can help to provide a model that has more meaningful properties in terms of the behaviour of the model itself.

[13] The results of the computations did not differ greatly for other choices made.

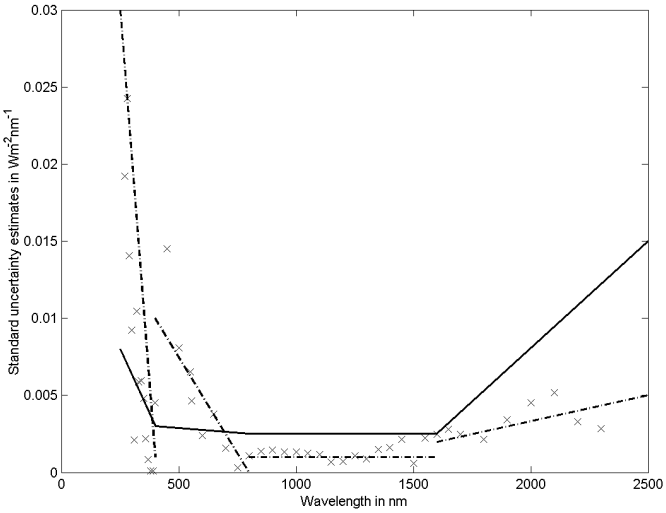

Figure 21: The crosses denote estimates of the standard uncertainties associated with the FEL196 spectral irradiance data obtained using local polynomial models. The broken straight lines represent a segmented standard uncertainty profile based on these estimates. The specified standard uncertainty profile is indicated by solid straight-line pieces.

uncertainty is not very efficient, i.e., as an *individual* value it might not be very reliable. However, taken together it is plausible that the set of estimates provides a reasonable indication of a "standard uncertainty profile" for the data.

It is therefore appropriate to replace the individual values by "smoothed" values. The manner in which to obtain suitably smoothed values is itself a modelling exercise comparable in difficulty to modelling the data itself. For current purposes, the data range was subdivided in accordance with the breakpoints in table 1, and over each subdivision the standard uncertainty taken as varying linearly with wavelength. This choice was made because (a) a different instrument was used to provide the measurements in each subinterval, and (b) the original specification of the uncertainties was linear in each subinterval. The linear variations were chosen by eye[14] and are depicted in figure 21 by broken straight-line segments. For comparison, the specified standard uncertainty profile (table 1) is shown in the figure as solid straight-line pieces.

There are some inconsistencies between the provided uncertainties and those estimated as above. Generally, the specified uncertainties at the lower end of the spectral region would appear to be too low, whereas those for the bulk of the region seem to be too large.

[14]Such a choice could be automated, but it would be difficult to do so. One reason is that a linear piece might predict a very small or even a negative standard uncertainty, which would be physically meaningless.

A Planck-polynomial model based on these estimated uncertainties differs little in its behaviour from the model for the provided uncertainties. Visually, it appears identical to that in figure 5, but the associated uncertainties are different.

Table 3 gives the counterpart of table 2 for the weighted root-mean-square residuals s_n for polynomial orders $n = 1$ to 20. The values of s_n for small n are somewhat different from those obtained previously, but again they saturate to a value close to unity, indicating the consistency of the model and the data, as before. The difference lies in the distribution of the weighted residuals themselves: see figure 22, which should be compared with figure 6. There is no extreme residual at $\lambda = 270$ nm as previously. There is a somewhat less extreme value at $\lambda = 1450$ nm.

Polynomial order n	1	2	3	4	5	6	7	8	9	10
RMS wt. residual s_n	24.7	10.2	7.4	5.5	3.4	2.1	1.8	1.6	1.3	1.1
Polynomial order n	11	12	13	14	15	16	17	18	19	20
RMS wt. residual s_n	0.9	0.8	0.8	0.9	0.9	0.9	0.9	0.9	0.9	0.9

Table 3: The root-mean-square (RMS) weighted residual s_n (non-dimensional) for the Planck-polynomial model as a function of polynomial order n for lamp FEL196. The uncertainties associated with the data that were used were those described in section 5.6, rather than those provided.

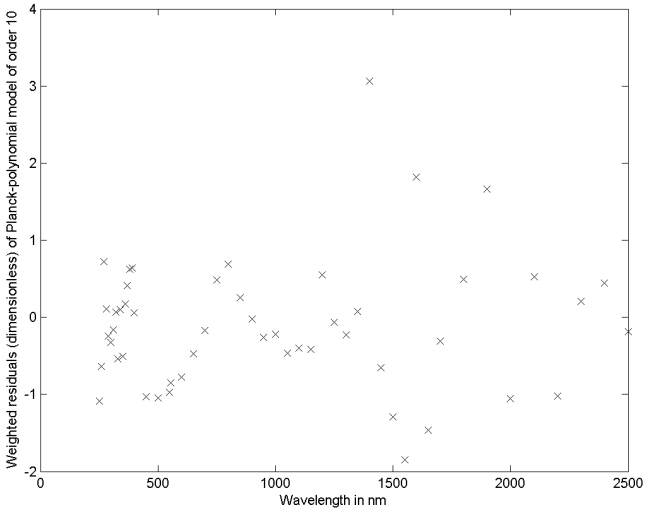

Figure 22: The weighted residuals for the Planck-polynomial model of order $n = 10$ when the uncertainties associated with the data are estimated as described in section 5.6, rather than those provided.

The unweighted model residuals and the 95 % uncertainty swathe are depicted in figure 23, for comparison with figure 7. Although the standard uncertainty profile (broken straight line in figure 21) appears to be a reasonable summary of

the estimated standard uncertainties (crosses in figure 21) a greater number of the unweighted residuals in figure 23 lie outside the 95 % uncertainty swathe (although they largely fall into groups).

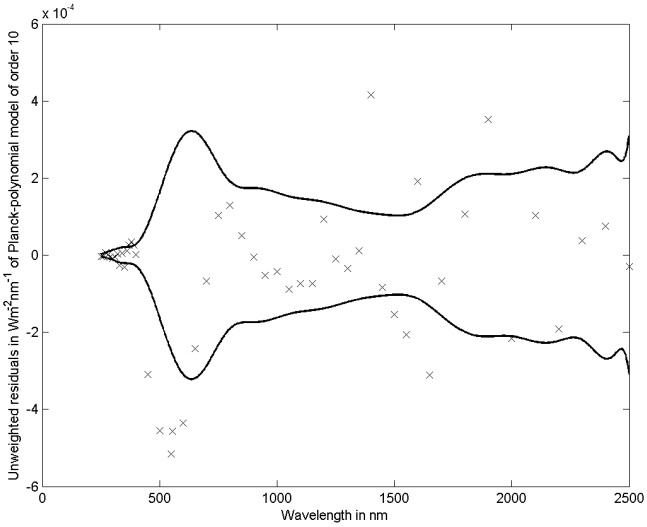

Figure 23: The unweighted residuals for the Planck-polynomial model of order $n = 10$ and the 95 % uncertainty swathe when the uncertainties associated with the data are estimated as described in section 5.6, rather than those provided.

5.7 Uncertainty associated with integrated quantities

Many applications of optical radiation metrology require a calculation of an integrated quantity and the associated uncertainty. One of the most important uses for the models developed here would be to obtain this uncertainty.

The most straightforward example is the uncertainty associated with an estimate of the total irradiance of a source, obtained by integrating over the spectral region the spectral irradiance model considered here.[15] For instance, a large-area radiance source has been developed at NPL [21] and was used to calibrate the GERB instrument, which will measure the Earth radiation budget from a geostationary orbit [19].[16] The source was calibrated for spectral radiance at NPL in a similar manner to which the lamps that have been modelled in this work were calibrated, providing radiance at a set of discrete wavelengths. Because the GERB instrument

[15] Since the model applies only to the region spanned by the available data, this "total irradiance" relates to this range of wavelengths. The model is not capable of extrapolation to the remaining wavelengths because it is not based purely on physical considerations. It would be necessary to estimate by other means the contribution attributed to these wavelengths.

[16] See www.ssd.rl.ac.uk/gerb

measures *total* radiance, it was necessary to determine the *integrated* radiance of the source, and the uncertainty associated with this integrated value, from the set of discrete values. An estimate of the integrated radiance was obtained by applying a quadrature rule to these values. It was necessary to make certain assumptions in evaluating the uncertainty associated with the provided estimate of the integrated radiance. The model considered would provide a better basis for both the integration and the associated uncertainty.

The general principle involved here is that the parameter estimates $\widehat{\mathbf{a}}$ that define the polynomial part of the model have an associated uncertainty matrix $V_{\widehat{\mathbf{a}}}$ (section 2.3). Together with the uncertainties associated with any other inexactly known quantities that appear in the integrand, the influence of these effects on the uncertainties associated with the values of the integral can be evaluated using the law of propagation of uncertainty [4]. The fact that the $\widehat{\mathbf{a}}$ are mutually dependent, because they are derived from the same data (the values of E_i and the associated uncertainties), is crucial. Were these dependencies not taken properly into account by applying the law of propagation of uncertainty *with a full set of covariance terms*, the resulting uncertainties would be invalid.

5.7.1 Filter radiometer (radiation thermometer) measurements of a black body

The spectral radiance of a black body is described by the Planck function, which is a function of temperature (and wavelength) only. Two methods are commonly used to measure the temperature of a black body source, and both rely on a measurement with a spectrally selective detector of part of the Planck function.

In radiometry, an absolute measurement of thermodynamic temperature is made using a filter radiometer. The filter radiometer is calibrated for spectral responsivity over its entire response range. The signal V_{FR} expected in the filter radiometer is given by

$$V_{\mathrm{FR}} - V_{\mathrm{OOB}} = sG\epsilon g\pi R \int_0^\infty r(\lambda)\tau(\lambda)L(\lambda;T)d\lambda, \tag{29}$$

where V_{OOB} is the out-of-band signal, s the size of source effect, G the amplifier gain, ϵ the black body emissivity, g the geometric factor, R the absolute responsivity of the filter radiometer, $r(\lambda)$ the relative spectral responsivity of the filter radiometer, $\tau(\lambda)$ the transmission of the lens (when used), and $L(\lambda;T)$ the spectral radiance of the black body at the temperature T in air, which is given by Planck's equation (1).

Equation (29) can be solved using numerical techniques to give the temperature from the measured signal V_{FR}.

In thermometry, temperature is defined according to the ITS-90 practical tempera-

ture scale. Above the freezing point of silver, temperature is defined using Planck's radiation law and the melting temperature of any one of the silver, gold or copper points. This is realised using radiation thermometers and the ratio

$$\frac{L(\lambda;T_{90})}{L(\lambda;T_{90}(X))} = \frac{e^{\beta/(\lambda T_{90}(X))}-1}{e^{\beta/(\lambda T_{90})}-1}, \tag{30}$$

where $\beta = hc/(nk)$ (see (1)), and $T_{90}(X)$ is the freezing temperature of any of those metals.

Radiation thermometers, also known as pyrometers, are used to realise the temperature scale above the silver point. From (30), an ideal radiation thermometer would have an extremely narrow bandwidth and generally this is achieved by using an interference filter along with a Si photodiode or a photomultiplier.

Physically radiation thermometers are very similar to filter radiometers, but they differ in two important aspects: the focusing optics forms part of the radiation thermometer and can consist of lenses or focusing mirrors and, more fundamentally, they differ from filter radiometers in the way that they are calibrated.

A filter radiometer is calibrated radiometrically with the purpose of defining its spectral responsivity. This spectral responsivity is then used to measure the thermodynamic temperature of the black body according to (29). A radiation thermometer however is defined according to the ratio in (30). In practice, because of the finite bandwidth of the radiation thermometer, the ratio actually measured is

$$\frac{\int_0^\infty S(\lambda)L(\lambda;T_{90})d\lambda}{\int_0^\infty S(\lambda)L(\lambda;T_{90}(X))d\lambda}, \tag{31}$$

where $S(\lambda)$ is the spectral responsivity of the entire thermometer (including the transmittance of the optics and the interference filter and the responsivity of the detector). Since in practice this makes it difficult to solve for temperature, various methods have been developed to reduce the required numerical integration. The most common method is to define an effective wavelength for the radiation thermometer. This effective wavelength, calculated at approximately the correct temperature, can then be used in place of the monochromatic wavelength in (30). The effective wavelength is defined by

$$\lambda_{\text{eff}} = \frac{\int_0^\infty \lambda S(\lambda)L(\lambda;T_{90})d\lambda}{\int_0^\infty S(\lambda)L(\lambda;T_{90})d\lambda}. \tag{32}$$

Use of the effective wavelength simplifies the equations, but as with any approximation, introduces its own uncertainties. Since computers have been available it is as easy to use the full equations. However, this approximation is still useful for estimating uncertainties, for example those due to incorrect measurements of the spectral responsivity of the detector.

The modelling methods developed here can be used to model the spectral responsivity of the filter radiometer or radiation thermometer. This allows the calculation of temperature according to (30) to be made more easily without requiring the effective wavelength. It will also be of value in determining the uncertainties associated with both the radiometric and thermometric determinations of temperature.

5.8 Filter radiometer measurements of lamps

Possible work on the filter radiometer measurements of lamps is an extension of that of the previous section, where the integral is determined of the filter radiometer responsivity weighted by a Planck function. The Planck function itself is defined rather than estimated and there is therefore no uncertainty associated with that source. This section describes the use of a filter radiometer to measure a lamp, which has its own associated uncertainty in spectral irradiance.

For example, if it is only possible to measure relative spectral radiance or irradiance of a source (cf. section 5.4), it is necessary to convert these results into absolute measurements. Thus, a multiplicative factor is to be determined to apply to the entire relative spectrum. For this purpose, a set of filter radiometers is typically used to measure the source.

For an irradiance source measured with a filter radiometer, the expected signal is

$$V = GR \int_0^\infty r(\lambda) E_{\mathrm{lamp}}(\lambda) d\lambda,$$

where G is the amplifier gain, R the filter radiometer absolute responsivity, $r(\lambda)$ the filter radiometer relative spectral responsivity, and $E_{\mathrm{lamp}}(\lambda)$ the irradiance of the lamp.

For a radiance source

$$V = sGg\pi R \int_0^\infty r(\lambda) \tau(\lambda) L_{\mathrm{source}}(\lambda) d\lambda,$$

where s is the size of source effect, G the amplifier gain, $\tau(\lambda)$ the lens transmission, g the geometric factor between the lens and filter radiometer apertures, $r(\lambda)$ the filter radiometer spectral responsivity, and $L_{\mathrm{source}}(\lambda)$ the radiance of the source.

Each filter radiometer has a measured spectral responsivity and associated spectral uncertainty, as modelled in the current work. Similarly, the source has a model for its spectral irradiance and associated spectral uncertainty. Numerical integration over the bandwidth of the filter radiometer of the multiple of the source and filter radiometer will give the expected signal in the filter radiometer. This result can be compared with the measured signal.

A useful extension would be to calculate the best multiplicative factor given a range of different filter radiometer measurements (usually at a range of wavelengths), taking into account the uncertainty associated with both the lamp and filter radiometer measurements, and to evaluate the uncertainty associated with that factor.

5.9 Using photometers with non-tungsten sources

One important type of filter radiometer is a photometer. A photometer is designed so that its spectral responsivity matches as closely as possible the so-called $V(\lambda)$ curve, which represents the human eye response. Photometers are used because they can supply photometric results with one straightforward measurement. Thus, the lamp does not need to be spectrally calibrated.

However, a real photometer will not perfectly match the theoretical $V(\lambda)$ profile. To take account of this fact, a colour correction factor is applied. The correction must be weighted to the lamp being measured, since an error in the part of the spectrum where the lamp has low output is less important than an error in the part of the spectrum where the lamp has a high output. The colour correction factor is the ratio of (a) the integral of the product of the lamp profile and the ideal $V(\lambda)$ profile, and (b) the integral of the product of the lamp profile and the actual responsivity profile of the photometer.

Commonly, a photometer is calibrated using a tungsten lamp, and a colour correction factor is applied for this lamp. If subsequently it is used to measure a different tungsten lamp, the colour correction factor will be similar. However, for a highly spectrally varying source, such as an LED or a discharge source, the colour correction factor will be very different since these sources often have peaks in output exactly where the photometer least matches the required profile.

The techniques developed in this work could be extended to address such issues. Since a photometer is a type of filter radiometer, its spectral responsivity can be modelled by these methods. It would then be necessary to produce a spectral model for the lamp. This model would probably have to be in a different form, since these lamps are, by definition, spectrally different from the Planckian-like lamps modelled here, although their spectral shape will in general more easily be physically defined than the filter radiometers modelled in this study. These models could then be used to calculate the colour correction factor for the photometer-lamp combination and to calculate the uncertainty associated with it and with the photometric measurement.

With the more straightforward tungsten lamps, a colour correction factor is made for one tungsten lamp and then used for other lamps that may have a slightly different colour temperature and spectral shape. These models would be useful in evaluating the uncertainty associated with the estimate of the photometric quantity

due to using a colour correction factor calculated for a slightly different lamp. By measuring, and modelling, a large number of similar sources, say red LEDs, it should be possible to quantify the extent to which a generic colour correction factor could be applied for photometric measurements of all such LEDs.

5.10 Key comparisons involving spectral quantities

One of the biggest challenges facing the implementation of the Mutual Recognition Arrangement (MRA) [3] is the treatment of the results of key comparisons having a spectral dimension. In this regard, a valuable approach would be to model "simultaneously" as a function of wavelength the data provided by all participants in the comparison, accounting for their stated uncertainties. By so doing it can be expected that the resulting model curve would be a more realistic and potentially smoother realisation of the underlying spectral characteristic than would be provided by the results of any single participant. Because of the greater redundancy of data the consequent uncertainty swathe (section 2.3) would be narrower.[17] Should the approach be adopted in future work, there would be benefit in tailoring some of the generic approaches on *key comparison reference curves* (KCRCs) being developed as part of the NMS Software Support for Metrology programme and by BIPM Director's Advisory Group on Uncertainty [10, 11]. The approach described here is potentially capable of application to an aggregation of the data provided by the participating laboratories, even if they do not necessarily provide measurements at the same wavelengths or at the same number of wavelengths. The successful provision of KCRCs would help to meet a number of identified needs, including those identified by the CCPR Key Comparison Working Group and the CCT Working Group on Radiation Thermometry.

5.11 Efficient industrial re-calibration

Following initial calibration by a national measurement institute, typically at a large number of closely-spaced wavelengths, industrial laboratories provide re-calibrations of source and detector responses as part of their service to their customers. Typically, these laboratories do not possess facilities to measure the characteristics at more than a relatively small number of wavelengths, e.g., detector calibrations can only be made at a few fixed laser wavelengths. Even if laboratories had the facility, detailed re-calibration is expensive and can be labour-intensive.

Between the initial and subsequent calibrations it can be expected that the char-

[17] As with all key comparison data evaluations, should there be mutual dependencies between the participants' measurements, perhaps due to some of them taking traceability from a common source, it would be necessary to take account of them in the modelling. Otherwise, the uncertainty swathe would be optimistically narrow.

acteristic will change due to various effects. For instance, in the case of a source these effects would include lamp ageing, filament geometry changes, and changes in applied current. In itself, the measurement of the spectral characteristic at the time of re-calibration at a small number of wavelengths is unlikely to be adequate to model the characteristic sufficiently well. However, the magnitude of the *change* in the spectral characteristic between the original and a subsequent calibration can typically be expected to be much smaller than that of the characteristic itself. Therefore, if the change *varies smoothly* with wavelength, it might well be possible to model it by a relatively uncomplicated function having a small number of adjustable parameters. (If the change is *not* smoothly varying with respect to wavelength, a small amount of data would be insufficient to model the characteristic adequately. In this case no sensible re-calibration, made by a laboratory with limited facilities, that was valid across the relevant part of the spectrum would be possible *by any means* for such data.)

The resulting spectral characteristic at the time of re-calibration would take the form of the sum of two functions, one being the model of the characteristic at the time of the initial calibration and the other the model of the change. Further work could develop a procedure for industrial re-calibration based on this approach.

5.11.1 Detector-stabilised sources

The idea of re-calibrating a source at only a few wavelengths can be extended to the concept of detector stabilisation. Detector-stabilised lamps and large-area radiance sources have been developed at NPL as possible new transfer standards. Here the "re-calibration" can occur during operation of the lamp and form part of the transfer standard itself. The lamp is monitored by a set of filter radiometers at different wavelengths. One of these radiometers is held constant by an active feedback loop that changes the lamp current. This procedure significantly increases the usable time between full re-calibrations of the source. The other monitor channels check for any spectral shift of the source. If the spectral shift is greater than desired, the user can automatically be alerted to have the source returned for calibration. As a result, unnecessary calibration is prevented, and any changes in transportation that might otherwise go unnoticed are recorded.

Development of the methods described in sections 5.7.1 and 5.11 would improve the use of these monitor channels. If the spectral responsivity of the filter radiometers had previously been measured and monitored, any change in the monitor filter radiometers could be used to correct the original source calibration and give an up-to-date calibration for the lamp each time it was used.

5.11.2 Detector characterisation

Further to the above considerations, it would be valuable to investigate the extent to which detectors from any specific manufacturer can be characterised. Such a characterisation could be provided by a national measurement institute carrying out a detailed calibration and modelling of a small number, say three, detectors. The manufacturers would use this information, together with smaller numbers of subsequent measurements, to learn more about the properties of detectors of this type.

5.11.3 Optimal wavelengths

An additional possibility would be to use models such as those considered here to identify a set of wavelength values that are especially effective for re-calibration purposes. Such a set, which can be regarded as *pivotal* wavelengths, would constitute those that are the most influential in terms of defining the spectral "change" function. They would be pivotal in the sense that the resulting uncertainties would be smaller than those for other choices. An essential practical consideration would be that a number of specific wavelengths can be realised more readily than others. Hence, the best choice from *this* set would be the objective in this regard.

In the case of a detector stabilised source this approach would help to select the optimal filter radiometers to use for the monitor channels.

In addition, routine calibrations at national measurement institutes could be improved. At the moment it is difficult to decide the incremental wavelengths at which a lamp should be calibrated. A lamp measured at too few wavelengths is not properly characterised. For example, the SRIPS facility at NPL takes one hour to make measurements at a 5 nm spacing and ten minutes to make them at a 50 nm spacing. If too many wavelengths are chosen, lamps are less efficiently calibrated. It would be useful and straightforward to take a lamp that has been calibrated at a 5 nm spacing and make a model and uncertainty evaluation using (a) all the points, and the subset of these points at (b) a 20 nm spacing, (c) a 50 nm spacing, and (d) a 100 nm spacing, and compare the models produced in cases (a)–(d). By so doing, information would be provided on the wavelength spacing necessary to characterise that lamp fully. Obviously for each type of lamp the number of wavelength values necessary may differ. Moreover, there may be some spectral regions that require more measurements than others. However, generally measurements are made only of a few types of standard lamps, and hence this work would show in how much detail these lamps should be measured and provide a method for interpolating to intermediate wavelengths.

6 Conclusions

Approaches to the modelling of the spectral characteristics of sources and detectors have been described. These approaches have combined flexible empirical models with available physical knowledge of these characteristics. The consequences were models that were shown to have potential in the area of optical radiation metrology.

A particular aspect covered was the choice of model in any particular case from a "family" of candidate models. Model uncertainties were derived in a generic manner.

Spectral characteristics are typically obtained using an instrument that provides values integrated over a wavelength band rather than at a point value of wavelength. In order to accommodate this effect, the influence of the integration was studied in detail. Formulae were derived that permitted the indicated integrated values to be corrected to those that would be obtained using an instrument that passed only a single wavelength, that corresponding to the spectral point of interest.

A number of future work items relevant to optical radiation metrology based on the use of the models addressed here was indicated.

The work was supported by the National Measurement System Directorate of the UK Department of Trade and Industry as part of its NMS Software Support for Metrology (SS*f*M) programme.

References

[1] G. Andor. Approximation function of spectral irradiance of standard lamps. *Metrologia*, 35:427–429, 1998.

[2] H. M. Anthony and P. M. Harris. Polynomial fitting to noisy data where subsets of the data are subject to unknown vertical shifts. Technical Report DITC 136/88, National Physical Laboratory, Teddington, UK, 1988.

[3] BIPM. Mutual recognition of national measurement standards and of calibration and measurement certificates issued by national metrology institutes. Technical report, Bureau International des Poids et Mesures, Sèvres, France, 1999.

[4] BIPM, IEC, IFCC, ISO, IUPAC, IUPAP, and OIML. Guide to the Expression of Uncertainty in Measurement, 1995. ISBN 92-67-10188-9, Second Edition.

[5] R. P. Brent. *Algorithms for Minimization without Derivatives*. Prentice-Hall, Englewood Cliffs, New Jersey, 1973.

[6] C. W. Clenshaw. *Mathematical Tables Volume 5. Chebyshev Series for Mathematical Functions*. Her Majesty's Stationery Office, 1962.

[7] C. W. Clenshaw and J. G. Hayes. Curve and surface fitting. *J. Inst. Math. Appl.*, 1:164–183, 1965.

[8] M. G. Cox. Piecewise Chebyshev series. *Bull. Inst. Math. Appl.*, 22:163–166, 1986.

[9] M. G. Cox. Constructing and solving mathematical models of measurement. In P. Ciarlini, M. G. Cox, F. Pavese, and D. Richter, editors, *Advanced Mathematical Tools in Metrology II*, pages 7–21, Singapore, 1996. World Scientific.

[10] M. G. Cox. The evaluation of key comparison data. *Metrologia*, 39:589–595, 2002.

[11] M. G. Cox. The evaluation of key comparison data: An introduction. *Metrologia*, 39:587–588, 2002.

[12] M. G. Cox, P. M. Harris, and P. D. Kenward. Fixed- and free-knot univariate least-squares data approximation by polynomial splines. Technical Report CMSC 13/02, National Physical Laboratory, Teddington, UK, 2002.

[13] L. M. Delves and J. Walsh. *Numerical Solution of Integral Equations*. Clarendon Press, Oxford, 1974.

[14] P. E. Gill, W. Murray, and M. H. Wright. *Practical Optimization*. Academic Press, London, 1981.

[15] D. R. Hartree. *Numerical Analysis*. Clarendon Press, Oxford, 1958.

[16] J. G. Hayes. Curve fitting by polynomials in one variable. In *Numerical Approximation to Functions and Data*, pages 43–64, London, 1970. Athlone Press.

[17] JCGM. Guide to the Expression of Uncertainty in Measurement. Supplement 1: Numerical Methods for the Propagation of Probability Distributions. Technical report, Joint Committee for Guides in Metrology, 2002. Draft.

[18] P. Kärhä, P. Toivanen, F. Manoochehri, and E. Ikonen. Development of a detector-based absolute irradiance scale in the 380–900 nm spectral range. *Applied Optics*, 36:8909–8918, 1997.

[19] R. Mossavati, J. E. Harries, S. J. Kellock, R. T. Wrigley, J. Mueller, and N. P. Fox. Radiometric calibration of the GERB instrument. *Metrologia*, 35:603–607, 1998.

[20] W. Pogorzelski. *Integral Equations and their Applications, Volume 1*. Pergamon, Oxford, 1966.

[21] E. R. Woolliams, T. M. Hunt, N. J. Harrison, S. A. Windsor, N. P. Fox, J. R. Mountford, L. J. Rogers, and H. M. Pegrum. Improved transfer standard sources for calibration of field spectrometers used for Earth observation applications. *Sensors, Systems and Next-generation Satellites VI: Proceedings of SPIE*, 4881:386–394, 2003.

A Simultaneous determination of the colour temperature and the parameters of the Planck-polynomial model

This appendix addresses the statement made in section 2.1 concerning the unsuitability of modelling spectral irradiance data by the model (2) by *simultaneously* determining the colour temperature T in the Planck function $L(\lambda;T)$ and the parameters $\mathbf{a}$ of the multiplicative polynomial $G(\lambda;\mathbf{a})$, where $L(\lambda;T)$ is defined by equation (1) and $G(\lambda;\mathbf{a})$ is a polynomial of order n (degree $n+1$). The parameters T, $\mathbf{a}$ and n are to be determined.

For a prescribed polynomial order n, the modelling problem *can* be expressed as

$$\min_{T,\mathbf{a}} \sum_{i=1}^{m} \left(\frac{y_i - F(\lambda_i;T,\mathbf{a})}{u(y_i)} \right)^2 . \tag{33}$$

This problem can in principle be solved for successively increasing values of n, viz., for $n = 1, 2, \ldots$, until a satisfactory solution is obtained. However, this set of problems becomes increasingly poorer conditioned and the estimates of the parameters (both T and $\mathbf{a}$) poorer defined as n increases. The reason is that once n is sufficiently large for an acceptable solution, it is possible to perturb the value of T so obtained and determine a polynomial *of the same order* that gives a function F that is almost as good. Statistically, the polynomial parameters $\mathbf{a}$ become highly correlated with the colour temperature T.

Intuitively, the above observation can be expected. The Planck function determined in accordance with the definition of section 2.4 accounts for the general behaviour of the spectral irradiance data. The polynomial acts, as planned, as a correction to that Planck function. A slightly different Planck function, as a consequence of a neighbouring choice of colour temperature, will require a slightly different correction polynomial.

The procedure recommended in section 2.1, in which T is determined first, followed by the values of $\mathbf{a}$, is by comparison not optimal, but provides a stable solution. The extent of the lack of optimality appears to be negligible in the context of the magnitudes of the data uncertainties.

B Derivation of Planck-polynomial model uncertainties

Consider the *pure* polynomial model $G_n(\lambda; \mathbf{a})$ (expression (6)). Let $V_{\mathbf{E}}$ denote the covariance matrix associated with the measurements $\mathbf{E} = (E_1, \ldots, E_m)^{\mathrm{T}}$. For the current problem, in which var$(E_i) = u^2(E_i)$ and the covariance terms are zero, $V_{\mathbf{E}}$ is an $m \times m$ (diagonal) matrix with diagonal elements $u^2(E_i)$, $i = 1, \ldots, m$. Let J denote the $m \times n$ matrix of polynomial basis functions evaluated at the data points, i.e., with elements

$$J_{i,j} = T_{j-1}(x_i), \qquad j = 1, \ldots, n, \qquad i = 1, \ldots, m, \tag{34}$$

where

$$x_i = \frac{(\lambda_i - \lambda_{\min}) - (\lambda_{\max} - \lambda_i)}{\lambda_{\max} - \lambda_{\min}}, \qquad \lambda_{\min} = \min_r \lambda_r, \qquad \lambda_{\max} = \max_r \lambda_r.$$

The uncertainty matrix (covariance matrix) $V_{\widehat{\mathbf{a}}}$ associated with $\widehat{\mathbf{a}}$ is obtained [9] as

$$V_{\widehat{\mathbf{a}}} = (J^{\mathrm{T}} V_{\mathbf{E}}^{-1} J)^{-1}. \tag{35}$$

The presence of the Planck function acting as a multiplicative factor for $G_n(\lambda; \mathbf{a})$ implies that each term $T_{j-1}(x)$ in the polynomial basis, where x is given by formula (7), is multiplied by $L(\lambda; \widehat{T})$. The uncertainty matrix (35) still applies, except that the elements of J are now given by

$$J_{i,j} = L(\lambda_i; \widehat{T}) T_{j-1}(x_i), \qquad j = 1, \ldots, n, \qquad i = 1, \ldots, m,$$

rather than formula (34).

Quantities derived from the Planck-polynomial model depend on the estimates $\widehat{T}$ and $\widehat{\mathbf{a}}$. In turn the uncertainties associated with these quantities can be obtained from the uncertainties $u(\widehat{T})$ (appendix D) and $V_{\widehat{\mathbf{a}}}$ associated with $\widehat{T}$ and $\widehat{\mathbf{a}}$. In particular, suppose a derived quantity $h = h(\widehat{\mathbf{a}})$ depends *linearly* on $\widehat{\mathbf{a}}$, viz.,

$$h(\widehat{\mathbf{a}}) = \mathbf{q}^{\mathrm{T}} \widehat{\mathbf{a}},$$

where $\mathbf{q} = (q_1, \ldots, q_n)^{\mathrm{T}}$ is a vector of multipliers. Then [9], the standard uncertainty $u(h)$ associated with h is given by

$$u^2(h) = \mathbf{q}^{\mathrm{T}} V_{\widehat{\mathbf{a}}} \mathbf{q}.$$

If h also depends linearly on $\widehat{T}$, $\mathbf{q}$ would have one extra element and $V_{\widehat{\mathbf{a}}}$ would be replaced by $V_{\widehat{\mathbf{a}};\widehat{T}}$, viz., $V_{\widehat{\mathbf{a}}}$ augmented by an additional row and column, the only further nonzero entry being $u^2(\widehat{T})$ in position $(n+1, n+1)$. There are no covariance terms associated with $\widehat{T}$ and the elements of $\widehat{\mathbf{a}}$, since as stated $\widehat{T}$ is regarded as defined for the purposes of estimating $\mathbf{a}$. If $h(\mathbf{a})$ is a *nonlinear* function of $\mathbf{a}$, linearisation of h about $\mathbf{a} = \widehat{\mathbf{a}} = (\widehat{\mathbf{a}}_1, \ldots, \widehat{\mathbf{a}}_n)^{\mathrm{T}}$ is made and, for $j = 1, \ldots, n$,

q_j is taken as the partial derivative of first order of h with respect to a_j, evaluated at $\mathbf{a} = \widehat{\mathbf{a}}$. A statement similar to that above applies if h also depends on $\widehat{T}$.

An important case is when h is the value of the model $F_n(\lambda; \widehat{T}, \widehat{\mathbf{a}})$ at some λ, i.e.,

$$h = F_n(\lambda; \widehat{T}, \widehat{\mathbf{a}}) = L(\lambda; \widehat{T}) G_n(\lambda; \widehat{\mathbf{a}}). \tag{36}$$

Then, with x given by (7), the vector $\mathbf{q}$ is taken as the basis function values

$$L(\lambda; \widehat{T}) T_{j-1}(x), \qquad j = 1, \ldots, n.$$

Upon the application of the law of propagation of uncertainty [4], the standard uncertainty $u(F_n(\lambda; \widehat{T}, \widehat{\mathbf{a}}))$ associated with $F_n(\lambda; \widehat{T}, \widehat{\mathbf{a}})$ is given by

$$u^2(F_n(\lambda; \widehat{T}, \widehat{\mathbf{a}})) = L^2(\lambda; \widehat{T}) \boldsymbol{\phi}^{\mathrm{T}} V_{\widehat{\mathbf{a}}} \boldsymbol{\phi} + \left(\frac{\partial L}{\partial T}(\lambda; T)\bigg|_{T=\widehat{T}} G_n(\lambda; \widehat{\mathbf{a}}) \right)^2 u^2(\widehat{T}),$$

where

$$\boldsymbol{\phi} = (T_0(x), \ldots, T_{n-1}(x))^{\mathrm{T}}.$$

Using expression (3) and formula (1),

$$u^2(F_n(\lambda; \widehat{T}, \widehat{\mathbf{a}})) = L^2(\lambda; \widehat{T}) \boldsymbol{\phi}^{\mathrm{T}} V_{\widehat{\mathbf{a}}} \boldsymbol{\phi} + \left(\frac{\beta F_n(\lambda; \widehat{T}, \widehat{\mathbf{a}})}{\widehat{T}^2 (1 - \exp(-\beta/(\lambda \widehat{T}))} \right)^2 u^2(\widehat{T}).$$

When several quantities are to be derived from $\mathbf{a}$, they will generally be mutually dependent, because each such quantity will depend on all or some of the $\mathbf{a}$. Let the derived quantities be denoted by

$$\mathbf{h}(\mathbf{a}) = (h_1(\mathbf{a}), h_2(\mathbf{a}), \ldots)^{\mathrm{T}}.$$

Let H denote the matrix of partial derivatives of first order of the elements of $\mathbf{h}$ with respect to those of $\mathbf{a}$, evaluated at $\widehat{\mathbf{a}}$. The covariance matrix associated with $\mathbf{h}$ is

$$V_{\mathbf{h}} = H V_{\widehat{\mathbf{a}}} H^{\mathrm{T}}.$$

One use of this covariance matrix is in integration (section 5.7), where sums of the form

$$Q = \mathbf{g}^{\mathrm{T}} \mathbf{h} = \sum_r g_r h_r$$

are required. For this case,

$$u^2(Q) = \mathbf{g}^{\mathrm{T}} V_{\mathbf{h}} \mathbf{g}.$$

There is an extension, as above, when these quantities also depend on $\widehat{T}$.

C Colour temperature determination

In order to estimate the parameters T (and a_1) in accordance with the definition of colour temperature in section 2.4, it is first observed that at a minimum of

$$S = \sum_{i=1}^{m} \left(\frac{\epsilon_i}{u(E_i)} \right)^2, \qquad \epsilon_i = E_i - a_1 L(\lambda_i; T),$$

the partial derivatives of S with respect to T and a_1 are zero. Thus,

$$\sum_{i=1}^{m} \frac{\epsilon_i \partial \epsilon_i / \partial T}{u^2(E_i)} = \sum_{i=1}^{m} \frac{\epsilon_i \partial \epsilon_i / \partial a_1}{u^2(E_i)} = 0.$$

Introduce the shorthand notation

$$L_i(T) = L(\lambda_i; T), \qquad L_i'(T) = \frac{\partial L}{\partial T}(\lambda_i; T), \qquad L_i''(T) = \frac{\partial^2 L}{\partial T^2}(\lambda_i; T).$$

Since

$$\frac{\partial \epsilon_i}{\partial T} = -a_1 L_i'(T), \qquad \frac{\partial \epsilon_i}{\partial a_1} = -L_i(T),$$

it follows that at a minimum the estimates $\widehat{T}$ and $\widehat{a}_1$ of T and a_1 satisfy

$$\widehat{a}_1 \sum_{i=1}^{m} \frac{(E_i - a_1 L_i(\widehat{T})) L_i'(\widehat{T})}{u^2(E_i)} = 0 \tag{37}$$

and

$$\sum_{i=1}^{m} \frac{(E_i - \widehat{a}_1 L_i(\widehat{T})) L_i(\widehat{T})}{u^2(E_i)} = 0. \tag{38}$$

From equation (37), $\widehat{a}_1$ or the sum is zero. The former possibility can be discounted because the best approximation would be zero. From equation (38), $\widehat{a}_1$ can be expressed in terms of $\widehat{T}$, and thus written as

$$\widehat{a}_1(\widehat{T}) = \frac{\sum_{i=1}^{m} E_i L_i(\widehat{T}) / u_i^2(E_i)}{\sum_{i=1}^{m} L_i^2(\widehat{T}) / u_i^2(E_i)}. \tag{39}$$

Then, using equation (37),

$$F(\widehat{T}) \equiv \sum_{i=1}^{m} \frac{(E_i - \widehat{a}_1(\widehat{T}) L_i(\widehat{T})) L_i'(\widehat{T})}{u^2(E_i)} \tag{40}$$

is a function of $\widehat{T}$ that takes the value zero when $\widehat{T}$ equals the required colour temperature.

So the problem reduces to the solution of the nonlinear algebraic equation $F(\widehat{T}) = 0$, $F(\widehat{T})$ being specified by formula (40) with $\widehat{a}_1(\widehat{T})$ given by formula (39).

The partial derivative with respect to T of $L(\lambda;T)$, values of which are required in function (40), is

$$\frac{\partial L}{\partial T}(\lambda;T) = \frac{\alpha\beta\exp(\beta/(\lambda T))}{\lambda^6 T^2(\exp(\beta/(\lambda T))-1)^2}.$$

Approaches to the numerical solution of $F(T)=0$ include Newton-Raphson and secant, and safeguarded algorithms derived from these to avoid the possibility of divergence [5]. A simple but safe procedure, based on bracketing the solution and then applying bisection is recommended.

Use an initial estimate T_0 or, if no estimate is available, take $T_0 = 3000$ K (the precise choice is not critical). Form $T_{\min} = 0.9T_0$ and $T_{\max} = 1.1T_0$. Should $F(T_{\min})F(T_{\max}) < 0$, $[T_{\min}, T_{\max}]$ provides a bracket and bisection can be applied. Otherwise, use $T_{\min} = (0.9)^2 T_0$ and $T_{\max} = (1.1)^2 T_0$, etc.

Because the computation time is minimal compared, e.g., with producing the graph of $s(T)$ (below), "pure" bisection can be used and is recommended for its combination of simplicity and robustness.

It is informative to provide a graph of the root-mean-square residual

$$s(T) = \left\{ \frac{1}{m-2} \sum_{i=1}^{m} \left(\frac{E_i - \widehat{a}_1(T) L_i(T)}{u(E_i)} \right)^2 \right\}^{1/2}$$

as a function of T for $T \in [T_{\min}, T_{\max}]$ at a large number (say, 1000) uniformly spaced values of T. The graph would indicate the sensitivity of the solution with respect to T.

D Colour temperature uncertainty

The estimate $\widehat{T}$ of the colour temperature T depends on the spectral irradiance values E_i. The law of propagation of uncertainty [4], based on the use of linear terms in the Taylor-series expansion of the model for T as a function of the E_i, gives

$$u^2(\widehat{T}) = \sum_{i=1}^{m} \left(\frac{\partial T}{\partial E_i}\bigg|_{T=\widehat{T}} \right)^2 u^2(E_i). \tag{41}$$

Differentiating formula (40) with respect to E_i,

$$\frac{\partial F}{\partial T}\frac{\partial T}{\partial E_i} + \frac{\partial F}{\partial E_i} = 0,$$

giving $\partial T/\partial E_i$ and hence formula (41) becomes

$$u^2(\widehat{T}) = \left(\frac{\partial F}{\partial T} \right)^{-2}\bigg|_{T=\widehat{T}} \sum_{i=1}^{m} \left(\frac{\partial F}{\partial E_i}\bigg|_{T=\widehat{T}} \right)^2 u^2(E_i). \tag{42}$$

From formula (40),

$$\frac{\partial F}{\partial T} = \sum_{i=1}^{m} \frac{(E_i - a_1(T)L_i(T))L_i''(T) - (a_1'(T)L_i(T) + a_1(T)L_i'(T))L_i'(T)}{u^2(E_i)}, \tag{43}$$

where, from formula (39),

$$\begin{aligned} a_1'(T) &= \frac{\sum_{i=1}^m E_i L_i'(T)/u^2(E_i)}{\sum_{i=1}^m L_i^2(T)/u^2(E_i)} \\ &- \frac{2\left(\sum_{i=1}^m E_i L_i(T)/u^2(E_i)\right)\left(\sum_{i=1}^m L_i(T)L_i'(T)/u^2(E_i)\right)}{\left(\sum_{i=1}^m L_i^2(T)/u^2(E_i)\right)^2}. \end{aligned} \tag{44}$$

Also, from formula (40),

$$\frac{\partial F}{\partial E_i} = L_i'(T)/u^2(E_i). \tag{45}$$

Thus, $u(\widehat{T})$ can be formed from formula (42), where $\partial F/\partial T$ is given by formula (43), with $a_1'(T)$ by formula (44), and $\partial F/\partial E_i$ is given by formula (45).

E Slit functions and their analysis

A monochromator is a device that uses a diffraction grating (or prism) to disperse light according to wavelength. The angle at which light leaves the grating is a function of wavelength. In a Czerny-Turner monochromator, light enters the monochromator by a fixed entrance slit and is focused by a fixed mirror onto a grating. This grating diffracts the light onto another fixed mirror that focuses the light onto a fixed exit slit. By changing the angle of the grating, different wavelengths of light reach the exit slit and therefore the detector.

If the slits were infinitely thin, only one wavelength would be passed. Their finite size means that a range of wavelengths will pass through the exit slit.

A monochromatic source (e.g., a laser, which has a negligibly narrow bandwidth) illuminating the entrance slit evenly with this wavelength, when the grating is at the correct angle for that wavelength, will give an image of the entrance slit on the exit slit. When the grating is rotated slightly, that image will shift and there will be a lower throughput. As the grating is rotated, the output of the monochromator will be a triangular function, as the image of the entrance slit is moved across the exit slit. This triangle is known as the monochromator slit function. In practice, this function is known inexactly, because mirror aberrations mean the entrance slit is not perfectly imaged onto the exit slits. Moreover, there may be a small difference between the sizes of the two slits.

If the entrance slit is illuminated with white light, as during measurement, light with the central wavelength is formed into an image that completely overlaps the exit slit and light with close wavelengths forms images that partially overlap. So a weighted throughput is obtained. For instance, for a monochromator nominally at 500 nm, more light is passed within a narrow band centred on this wavelength, less within such a band centred on 499.9 nm, less still within such a band centred on 499.8 nm, and so on until below 497.5 nm, say, no light is passed. The effect is symmetric about 500 nm, and thus no light is passed for wavelength above 502.5 nm.

Because a typical lamp has an output power that varies with wavelength, the symmetric behaviour of the slit is weighted by the spectral irradiance function of the lamp. In addition, measurements usually involve comparing one source with another, and if these have different spectral shapes, for example where one is increasing and the other decreasing with wavelength, they will be differently affected by the slit function.

For sources, measurements are taken with a monochromator having a slit function of finite width. Rather than the spectral response being provided at a wavelength value λ, the value indicated corresponds to the response averaged over a range of values distributed about λ. The averaging is in a weighted sense, according to the nature of the slit function.

It is essential to quantify the effect of the finite width of the slit function. Does a slit of width less than, say, 10 nm have a negligible influence in that the value provided is identical, to within measurement uncertainty, to that which would be provided by a slit of zero width? What is the maximum slit width that would be acceptable in this regard? What uncertainty would result from the use of a measurement provided by a slit of finite width compared with a slit of zero width?

The treatment in appendix G provides answers to these questions in the case of a triangular slit. The case of a rectangular slit, arguably a practical worst case in terms of "wavelength spread" (the hypothetically worst case would be a U-shaped slit, but such a slit is physically unrealistic), introduces a "factor of two" effect compared with the triangular slit (appendix G).

F Fredholm integral equations of the first kind

A Fredholm integral equation of the first kind is an equation that can be expressed generally as

$$\int_a^b K(t,s)f(s)ds = g(t), \qquad a \le t \le b,$$

where $g(t)$ is a specified function and $K(t,s)$ a specified kernel. Its solution for $f(t)$ is one of the notoriously difficult problems in mathematical physics. A solution may not exist and, even if it does, a small change in the function $g(t)$ can induce an arbitrarily large change in the solution $f(t)$. Further, functions can exist that satisfy the equation closely, yet be far from the "true" solution. It is thus known as an "ill-posed" problem [13].

Since the function $g(t)$ is often specified inexactly, being based on measurement, the above difficulties are exacerbated. For the problem under discussion, the function(s) corresponding to $g(t)$ is indeed measured.

Because two Fredholm integral equations of the first kind are to be solved in the current application (section (3)), there would seemingly be even greater potential for numerical difficulties. However, as shown in appendix G, the fact that the kernel has compact support, in the form of a rectangular or symmetric triangular function, avoids this difficulty. The so-called "compact Fredholm" procedure considered there is therefore recommended for spectral problems involving measurements with instruments having narrow slit functions.

G The solution of Fredholm integral equations of the first kind with a rectangular or triangular kernel

Let $V(\lambda)$ denote a spectral response characteristic to be measured. V might be voltage, for example. Then, if $S(\lambda_0, \lambda)$ denotes the spectral characteristic of the monochromator slit function when used at $\lambda = \lambda_0$, the indicated value, in the absence of measurement error and other effects, is

$$\widetilde{V}(\lambda) = \frac{\int_0^\infty S(\lambda,\ell)V(\ell)d\ell}{\int_0^\infty S(\lambda,\ell)d\ell}.$$

The denominator term constitutes a normalisation constant equal to the area under the slit function. By scaling the slit function to have unit area,

$$\widetilde{V}(\lambda) = \int_0^\infty S(\lambda,\ell)V(\ell)d\ell,$$

the form used herewith.

Two types of slit function are analysed, a rectangular slit function and a triangular slit function. Other types can also be handled.

Consider first a rectangular slit function. Although such a form of slit function might be unrealistic in practice, an analysis based on it is not only simpler than for, say, a triangular slit function (below), but it also gives some insight into the nature and effects of a slit function.

A rectangular slit function (figure 24) of bandwidth $2\Delta\lambda$ and unit area centred on λ can be expressed as

$$S(\lambda,\ell) = \begin{cases} 1/(2\Delta\lambda), & \lambda - \Delta\lambda < \ell < \lambda + \Delta\lambda, \\ 0, & \text{otherwise.} \end{cases}$$

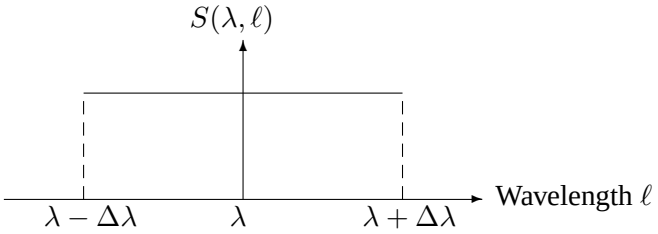

Figure 24: A rectangular slit function $S(\lambda,\ell)$ in the variable ℓ, centred on $\ell = \lambda$, with semi-width $\Delta\lambda$.

In the absence of measurement error and other effects, an instrument characterised by a such a slit function would indicate at λ the measurement

$$\widetilde{V}(\lambda) = \int_0^\infty S(\lambda,\ell)V(\ell)d\ell = \int_{\lambda-\Delta\lambda}^{\lambda+\Delta\lambda} \frac{1}{2\Delta\lambda}V(\ell)d\ell. \tag{46}$$

Of particular interest is the departure

$$e(\lambda) = \widetilde{V}(\lambda) - V(\lambda)$$

of $\widetilde{V}(\lambda)$ from $V(\lambda)$. To obtain $e(\lambda)$, first differentiate expression (46) with respect to λ:

$$\widetilde{V}'(\lambda) = \frac{V(\lambda+\Delta\lambda) - V(\lambda-\Delta\lambda)}{2\Delta\lambda}. \tag{47}$$

Define the operator

$$D \equiv \Delta\lambda\frac{d}{d\lambda}.$$

The Taylor expansion of the right-hand side of expression (47) gives

$$\widetilde{V}'(\lambda) = \frac{1}{\Delta\lambda}D\left\{1 + \frac{1}{6}D^2 + \frac{1}{120}D^4 + O(D^6)\right\}V(\lambda).$$

Applying D^{-1} to each side of this expression,

$$\widetilde{V}(\lambda) = \left\{1 + \frac{1}{6}D^2 + \frac{1}{120}D^4 + O(D^6)\right\}V(\lambda).$$

Formal inversion gives

$$\begin{aligned} V(\lambda) &= \left\{1 - \frac{1}{6}D^2 + \frac{7}{360}D^4 + \cdots\right\}\widetilde{V}(\lambda) \\ &\equiv \widetilde{V}(\lambda) - \frac{1}{6}(\Delta\lambda)^2\widetilde{V}''(\lambda) + \frac{7}{360}(\Delta\lambda)^4\widetilde{V}^{\mathrm{iv}}(\lambda) + \cdots. \end{aligned}$$

This expression permits the *required* characteristic $V(\lambda)$ to be recovered from the *indicated* characteristic $\widetilde{V}(\lambda)$ and the derivatives of this indicated characteristic.

It follows that if the indicated characteristic $\widetilde{V}(\lambda)$ can be satisfactorily modelled by a mathematical function, $V(\lambda)$ can be determined from this function and its derivatives. The construction of such a function is a main purpose of this work.

Now consider a symmetric triangular slit function (figure 25) of bandwidth $2\Delta\lambda$ and unit area centred on λ:

$$S(\lambda,\ell) = \begin{cases} (\ell - (\lambda - \Delta\lambda))/(\Delta\lambda)^2, & \lambda - \Delta\lambda < \ell < \lambda, \\ ((\lambda + \Delta\lambda) - \ell)/(\Delta\lambda)^2, & \lambda < \ell < \lambda + \Delta\lambda, \\ 0, & \text{otherwise.} \end{cases}$$

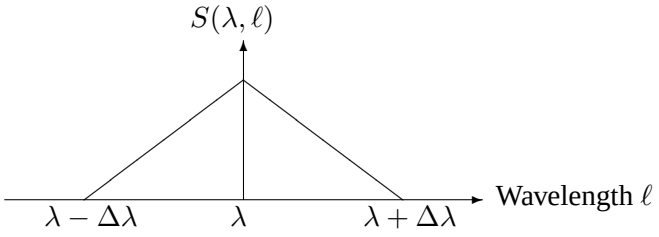

Figure 25: A triangular slit function $S(\lambda, \ell)$ in the variable ℓ, centred on $\ell = \lambda$, with semi-width $\Delta\lambda$.

The counterpart of the above rectangular-slit analysis is as follows. Now,

$$\widetilde{V}(\lambda) = \int_0^\infty S(\lambda,\ell)V(\ell)d\ell = I(\lambda,\Delta\lambda) + I(\lambda,-\Delta\lambda),$$

where

$$I(\lambda,\Delta\lambda) = \frac{1}{(\Delta\lambda)^2}\int_\lambda^{\lambda+\Delta\lambda}((\lambda+\Delta\lambda) - \ell)V(\ell)d\ell.$$

Since

$$\frac{\partial}{\partial\lambda}I(\lambda,\Delta\lambda) = \frac{1}{(\Delta\lambda)^2}\int_\lambda^{\lambda+\Delta\lambda}V(\ell)d\ell - \frac{1}{\Delta\lambda}V(\lambda),$$

it follows that

$$\begin{aligned} \widetilde{V}'(\lambda) &= \frac{1}{(\Delta\lambda)^2}\int_\lambda^{\lambda+\Delta\lambda}V(\ell)d\ell - \frac{1}{\Delta\lambda}V(\lambda) \\ &+ \frac{1}{(\Delta\lambda)^2}\int_\lambda^{\lambda-\Delta\lambda}V(\ell)d\ell + \frac{1}{\Delta\lambda}V(\lambda) \\ &= \frac{1}{(\Delta\lambda)^2}\int_\lambda^{\lambda+\Delta\lambda}V(\ell)d\ell - \frac{1}{(\Delta\lambda)^2}\int_{\lambda-\Delta\lambda}^{\lambda}V(\ell)d\ell, \end{aligned}$$

and thus

$$\widetilde{V}''(\lambda) = \frac{V(\lambda + \Delta\lambda) - 2V(\lambda) + V(\lambda + \Delta\lambda)}{(\Delta\lambda)^2}.$$

Hence, by analogy with the case of the rectangular slit,

$$\widetilde{V}(\lambda) = \left\{1 + \frac{1}{12}D^2 + \frac{1}{360}D^4 + O(D^6)\right\} V(\lambda),$$

giving

$$\begin{aligned} V(\lambda) &= \left\{1 - \frac{1}{12}D^2 + \frac{1}{240}D^4 + \cdots\right\} \widetilde{V}(\lambda) \\ &\equiv \widetilde{V}(\lambda) - \frac{1}{12}(\Delta\lambda)^2\widetilde{V}''(\lambda) + \frac{1}{240}(\Delta\lambda)^4\widetilde{V}^{\mathrm{iv}}(\lambda) + \cdots \end{aligned} \qquad (48)$$

and hence

$$e(\lambda) = \frac{1}{12}(\Delta\lambda)^2\widetilde{V}''(\lambda) - \frac{1}{240}(\Delta\lambda)^4\widetilde{V}^{\mathrm{iv}}(\lambda) + \cdots.$$

The leading term in this expression for $e(\lambda)$ is half that for the rectangular slit. It would indeed be expected that it would have a smaller magnitude because the triangular slit function gives a greater emphasis to values near its centre, whereas the rectangular slit function carries the same weight throughout its range.

If $\widetilde{V}(\lambda)$ has been modelled mathematically, the use of expression (48) will provide a mathematical form for $V(\lambda)$.

If the mathematical representation of $\widetilde{V}(\lambda)$ is available, as it would be from modelling, the higher-order terms in the series representation of $e(\lambda)$ can be determined to check whether they make a non-negligible contribution.

There are (at least) three ways in which the result (48) can be used:

1. As an estimate of the approximation error committed by using $\widetilde{V}(\lambda)$ in place of $V(\lambda)$. For this purpose a model of the data can be used to provide $\widetilde{V}''(\lambda)$ required in expression (48). If, for each value of λ at which a measurement is made, $|e(\lambda)|$ is negligible compared with the provided uncertainty, the effects of the slit function can be ignored and the indicated value regarded as a valid estimate of a point measurement at λ.

2. To *correct* $\widetilde{V}(\lambda)$ to estimate $V(\lambda)$:

   $$V(\lambda) \approx \widetilde{V}(\lambda) - \frac{1}{12}(\Delta\lambda)^2\widetilde{V}''(\lambda).$$

   Such a correction would be appropriate were $|e(\lambda)|$ not regarded as negligible.

3. As an input to instrument design. If a slit of a sufficiently small semi-width $\Delta\lambda$ were designed such that $|e(\lambda)|$ is negligible throughout the relevant spectral range, the slit function effects could be ignored.

Summary of procedure to obtain a corrected response (equivalent to one for a slit of zero bandwidth) from a measured response

1. Model the provided data (which constitutes measurements of $\widetilde{V}(\lambda)$) using the approach in section 2.1.

2. Use the model to obtain the error

$$e(\lambda) = \frac{1}{12}(\Delta\lambda)^2\widetilde{V}''(\lambda)$$

   in the indicated response.

   Note. Higher-order terms may be included if it is thought they are significant or it is not known whether they are significant.

3. If $|e(\lambda)|$ is negligible throughout the required spectral region compared with the uncertainty in the measurements of $\widetilde{V}(\lambda)$, no correction is necessary. Take

$$V(\lambda) = \widetilde{V}(\lambda)$$

   and the procedure is finished.

4. Form the corrected response

$$V(\lambda) = \widetilde{V}(\lambda) - e(\lambda).$$